Fundamental Study of Sterilization Effects on Marine *Vibrio* sp. in a Cylindrical Water Chamber with Supply of Only Underwater Shock Waves

Jingzhu Wang, Akihisa Abe, Yiwei Wang, Chenguang Huang

PII: S1350-4177(17)30563-1
DOI: https://doi.org/10.1016/j.ultsonch.2017.11.047
Reference: ULTSON 3984

To appear in: *Ultrasonics Sonochemistry*

Received Date: 27 October 2017
Revised Date: 28 November 2017
Accepted Date: 30 November 2017

Please cite this article as: J. Wang, A. Abe, Y. Wang, C. Huang, Fundamental Study of Sterilization Effects on Marine *Vibrio* sp. in a Cylindrical Water Chamber with Supply of Only Underwater Shock Waves, *Ultrasonics Sonochemistry* (2017), doi: https://doi.org/10.1016/j.ultsonch.2017.11.047

Fundamental Study of Sterilization Effects on Marine *Vibrio* sp. in a Cylindrical Water Chamber with Supply of Only Underwater Shock Waves

Jingzhu Wang*[(1)(2)], Akihisa Abe[(3)], Yiwei Wang[(1)(2)], Chenguang Huang[(1)(2)]
[(1)]Key Laboratory for Mechanics in Fluid Solid Coupling Systems, Institute of Mechanics, Chinese Academy of Sciences, No. 15 Beisihuanxi Road, Haidian Distinct, Beijing, 100190, China
[(2)]School of Engineering Science, University of Chinese Academy of Sciences, China
[(3)]Graduate School of Maritime Sciences, Kobe University, 5-1-1 Fukaeminami-machi, Kobe, 658-0022, Japan
* Corresponding Author's email:wangjingzhu@imech.ac.cn

Abstract

The effect of shock sterilization on Marine *Vibrio* sp. is investigated by carrying out a bio-experiment based on a bubble-shockwave interaction. In the experiments, underwater shock waves with different strength and frequencies are produced by a high-voltage power supply in a cylindrical water chamber. The bio-experimental results show marine *Vibrio* sp. is completely inactivated in a short time by a 1.0-Hz electric discharge. However, a high sterilization effect requires a strong and high frequency of the bubble motion, and it also depends on the lifetime of the bubble. Subsequently, by an experiment with an air gap to prevent the underwater shock waves entering the cell suspension, it is found that the introduction of a strong shock pressure is not entirely required to obtain the effective sterilization. On the other hand, the direct effect of the sterilization by rebound shock wave resulting from the bubble-shock wave interaction is examined in the experiments. The results suggest that free radicals mainly contribute to killing marine bacteria, and direct mechanical effects of the bubble motion are not responsible. In addition, the creation of the OH radical is indirectly confirmed by measuring the H_2O_2 concentration. Finally, the Herring equation is solved to investigate the condition of free radical generation when considering the effect of thermal conductivity at the bubble interface. As a result, the effective sterilization conditions based on the bubble-shock wave interaction are clearly obtained.

Keywords: Ship's ballast water, Bubble-shock wave interaction, Free radicals, Rebound shock wave, Sterilization effect, Cylindrical water chamber

1. Introduction

Underwater shock waves have been extensively applied in the fields of medical engineering, food sciences, material processing, and other industries. Takayama [1] tried to employ underwater shock wave focusing in an ellipsoidal reflector to develop an extracorporeal shock wave lithotripsy and found the generation of cavitation bubbles behind these shock waves. The collapsing motion of these cavitation bubbles could cause the tissue damage in the body. Hokamoto et al. [2] attempted to weld a thin aluminum plate onto a zirconia ceramic using regulated underwater shock waves. The metal plate was accelerated to about 800 m/s and the interface also showed a very high bounding strength in their study. To develop a non-thermal food preservation method using shock waves, Loske et al. [3] investigated the bactericidal effect of *Escherichia coli* in an electrohydraulic shock wave generator. They indicated that the reduction of bacteria was related closely to shockwave-induced cavitation bubbles. In the field of marine sciences, a shock sterilization method based on a shock wave-microbubble interaction was proposed to inactivate marine bacteria in the ballast water of a ship by Abe et al. [4]. A microbubble is defined as a smaller bubble than 50-μm diameter possessing unique properties such as a larger surface area to volume ratio, a slower rising velocity in the liquid phase, and minus electric charges on the surface. The concept of the shock sterilization method is shown in Fig. 1. After the passage of an incident shock wave, the collapses of the microbubbles are induced and they begin to shrink at sufficiently rapid speed. The temperature and pressure inside them increase dramatically with the compression. Simultaneously, the condensation of surface electric charges can produce free radicals, as stated by Takahashi [5]. At the final stage, microbubbles reach the minimum size, and the extreme conditions inside the bubbles can also destroy chemical bonds to release free radicals. Beneš et al. [6] found that these free radicals destroy the membrane lipids, DNA, and other essential cell components of microorganisms by strong oxidation reaction. After that, rebound shock waves are generated just as the microbubbles expand from the minimum. The pressures of the rebound shock waves can act strongly on marine bacteria near the microbubbles. Therefore, marine bacteria are inactivated physically and biochemically using this shock sterilization method, so that the method is thought to be an extremely safe and clean technique from the viewpoint of marine ecosystem.

Wang and Abe [7] carried out a bio-experiment of marine *Vibrio* sp. with the supply of microbubbles to clarify the effect of the shock sterilization method in an ellipsoidal water tank. They also pointed out that cavitation bubbles generated behind the underwater shock wave focusing have a potential for the sterilization of marine bacteria. To investigate the contribution of cavitation bubble, they used the propagation of shear wave in a narrow

water chamber to produce cavitation bubbles [8]. The bio-experimental results exhibited that all of marine bacteria were killed in several minutes, and a high sterilization effect could require a high pressure of incident shock wave. In other researches, Delius et al. [9] examined the effects of shock wave-gas bubble interaction on cell destruction at the minimum static excess pressures. The freed hemoglobin was identified as a marker of cell destruction. They noted that shock waves with an amplitude of 400 kPa induced membrane destruction and other biological effects. Lokhandwalla and Sturtevant [10] analyzed the interactions of red blood cells with shock-induced and bubble-induced flows in a shock wave lithotripsy, respectively. A crucial contribution of radial bubble motion to membrane deformation was confirmed by their work. Sundaram [11] investigated the viability of cells exposed to varying doses of acoustic energy using a suspension of 3T3 mouse cells and suggested that the critical strains of the membranes could be easily exceeded when the cells were exposed to microbubble-induced shock waves.

Given these backgrounds, considering the simplification and improvement of the shock sterilization method proposed by Abe et al. [4], a bio-experiment of marine *Vibrio* sp. is undertaken using underwater shock waves without the supply of microbubbles in a cylindrical water chamber. The underwater shock waves are generated by electric discharges with different strength and frequencies. Generation probability of cavitation bubbles behind underwater shock waves is analyzed by pressure measurement. The sterilization effects are discussed under different conditions. Firstly, we clarify the sterilizing potential of the bubbles in the cylindrical water chamber. Subsequently, the role of the bubble in the shock sterilization method is determined. Combining with the observation of a video camera, the generation mechanism of the bubble inducing an effective sterilization is investigated using different-material separators between the test chamber and the electric discharge chamber. Third is concerned with the role of the incident shock pressure in the shock sterilization method. An optical schlieren method is used to grasp the propagation behaviors of underwater shock wave in a cuboidal water chamber. Finally, the independent action of free radicals produced by the bubble-shock wave interaction is clarified for killing marine bacteria, and the concentration of H_2O_2 that is one of the products of chemical reaction of free radicals is measured. Furthermore, the generation condition of free radicals by the bubble motion, related to temperatures and pressures, are theoretically investigated using the Herring equation.

2. Bio-experimental Setup

Figure 2 shows a bio-experimental arrangement. The experimental system consisted of a cylindrical water chamber, a high-voltage power supply (HPS 18K-A, Tamaoki Electronics Co-Ltd), a pulse generator, a pressure transducer (Fiber Optical Probe Hydrophone: FOPH 2000, RP acoustic), and an oscilloscope (DS7054A, Keysight Technologies, Inc.). Incident underwater shock waves were generated by the electric discharges with different strength and frequencies. The pressure measurement was used to analyze the propagation behaviors of the shock waves. The incident shock waves are reflected at the inner wall, and concentrate at the central axis of the cylindrical water chamber. Cavitation bubbles are probably produced due to expansion region behind the concentration of the underwater shock waves. These bubbles interact with the reflected shock waves or the next coming incident shock wave, and immediately they start the motion of collapse. When they collapse, rebound shock waves and free radicals are generated, and eventually marine bacteria around them are killed. To investigate the effect of the shock sterilization, cell experiments were carried out based on the study by Wang and Abe [7]. A solution of Marine *Vibrio* sp. isolated from seawater was used as a specimen. Marine *Vibrio* sp. belongs to the same genus as *Cholera* in the ballast water of a ship but has no virulence. The procedures of the cell experiments are as follows. Samples were extracted from the cell suspension, diluted serially, and then spread on agar plates. The plates were incubated for 24 hours at 35 ℃. Finally, the cell viability in 1 ml was evaluated using the numbers of colony-forming cells on the agar plates on the basis of the dilution ratio. During the experiments, the state in the water chamber was observed by a video camera (HDC-TM45, Panasonic Corporation) of which recording speed was 30 fps. In addition, to attain the sterilization effect of only rebound shock wave in the shock sterilization, sodium L-ascorbate was added to the cell suspension to get rid of the action of free radicals.

Figure 3 shows a schematic and a photo of the experimental cylindrical water chamber. The external dimension of the water chamber was 90 mm in diameter and 120 mm in length. It consisted of two equivalent parts, namely, the upper part was a test chamber and the lower was an electric discharge chamber. The shape of each part was a cylinder of 30 mm in diameter and 30 mm in depth with a circular cone of a 30-mm diameter, and depth of the taper end was 6 mm. The volume of the test chamber was about 23 ml. Two parallel slots in the electric discharge chamber were equipped for the installation of electrodes. A slot with a 6.5-mm diameter at the top of the test chamber was designed for the setup of a probe of pressure transducer and for the sample extraction of marine bacteria. In the cell experiments, the electric discharge chamber and the test chamber were filled with the distilled water and the cell suspension of marine *Vibrio* sp., respectively, and thereby a silicone film of 0.1 mm thickness was used to separate the two chambers. Additionally, the upper end of the slot in the test chamber was covered with a rigid wall during the experiment.

3. Results and discussion

3.1 Sterilizing Potential in Cylindrical Water Chamber

Figure 4 shows a pressure profile at a 30-mm position of the central axis of the test chamber from the discharge point obtained with FOPH 2000. In the figure, the experimental data within 10 μs is affected by the light noise of the discharge flash. We observe the 1st shock wave produced by the underwater electric discharge at about 19 μs and the 2nd shock wave at about 27 μs, respectively. From the fact mentioned above, the 2nd shock wave is the concentration of the reflected shock waves being followed by an expansion region. Based on propagation velocity of underwater shock wave, about 1500 m/s, the 3rd shock wave is the reflection wave of the 1st shock wave at the bottom boundary of the electric discharge chamber. Some expansion regions are also observed around the 3rd shock wave. Cavitation bubbles are presumed to be produced in these regions, so that the pressure variation after 30 μs is affected by their collapses.

Figure 5 shows the peak pressures behind the incident shock wave fronts measured at 20, 30, 40, and 50 mm from the discharge point in the test chamber with and without the separator of a silicone film. The pressures decrease from about 7.5 MPa to 4.1 MPa without the separator while change from 6.9 MPa at 20 mm to 3.1 MPa at 50 mm in the case of the silicone film separator. Although silicone material is supposed to has almost the same acoustic impedance as water, those results show that it slightly prevents the propagation of the underwater shock waves. According to the previous work by Abe and Mimura [12], the pressures of the shock wave fronts are probably required higher than 100 MPa to kill marine *Vibrio* sp. Furthermore, Wang and Abe [13] also reported that the critical pressure destroying the cell membrane of marine *Vibrio sp.* was estimated to be about 150 MPa by their hybrid numerical method. Therefore, in the present experiment, it is not possible to directly inactivate marine bacteria only by the incident shock waves. On the other hand, it is thought that the critical pressure can be obtained when the shock pressure of over 3 MPa interacts with micron-sized bubbles. From the results in Figs. 4 and 5, the interactions of the cavitation bubbles with the shock pressures are expected to kill marine bacteria in the cylindrical water chamber.

Figure 6 shows an estimation of the number of viable cells at 31.6-kV electric discharges in the cylindrical water chamber. In the figure, the initial density of marine bacteria is about 4.62×10^4 cfu/ml. Solid squares with red curve represent the reference data of the cell suspension without triggering the electric discharge, i.e., without the action of shock waves. In this case, the number of viable cells hardly changes. Solid triangles with purple curve present the bio-experimental results estimated from the colony number of viable cells on the ager plates as shown in photos. Here, the electric discharge was triggered every second, i.e., the applied frequency was 1 Hz. The samples were taken from the test chamber at 30, 60, 70, 80, 90, and 100 seconds from the beginning of the bio-experiment, then diluted serially, and spread on the agar plates. The agar plates in photos show the results obtained by the same dilution. It shows that marine bacteria are killed completely in about 90 seconds.

Figure 7 shows estimates of the number of viable cells after an electric discharge of 35.1 kV to 18.8 kV. The frequency of the electric discharges was 1 Hz. Each symbol marked in this figure indicates of the averages for 10 sets of the bio-experimental data. Here, the error bars are not presented because the low values of the standard deviation (STD) are not clearly recognized in the exponential ordinate of the viable-cell number. In the figures including the following bio-experimental results, the STD are less than 12, even close to 0 except the point (STD ≈ 23) at the beginning of the experiments. This figure shows that marine bacteria are completely killed after about 70 seconds with an electric discharge of 35.1 kV. In the case of an 18.8-kV electric discharge, it takes about 190 seconds to attain perfect sterilization. Thus, the sterilization effects increase with the output power of the electric discharge, i.e., the collapses of bubbles are assumed to be enhanced by the output power of electric discharge. On the other hand, for the results obtained with an electric discharge of 30.0 kV to 18.8 kV, the gradients of the curves are found to be almost the same just in the first 30 seconds. This suggests that the sterilization effect of the bubble collapses is same during the first 30 seconds, although the strength of the incident shock pressures is different. Hence, we consider that there are only a few bubbles generated, so that the effective sterilizations are not represented during this period. Furthermore, we should note that the negative gradient of each curve is increasing gradually after every sample extraction, and therefore the number density of the bubbles is thought of increase.

Figure 8 shows estimates of the number of viable cells at the electric discharge of 31.6 kV under different applied frequencies of the shock waves. Solid triangles, diamonds, and squares represent the bio-experimental results of 1 Hz, 0.2 Hz, and 0.1 Hz, respectively. Other experimental conditions were similar to that in Fig. 7. The photos were obtained with an electric discharge of 1 Hz at 0, 30, and 60 shots. Due to the light refraction and low transparency of the cylindrical water chamber, the states in the chamber are slightly unclear. However, the generation of the bubbles is recognized by the change in the white area in the test chamber. From this figure, it is found that the complete sterilization is obtained after 90 shots of the electric discharges for a 1-Hz frequency while it takes about 180 shots for 0.1 Hz. The three curves in Fig.8 represent like convex profile, and their gradients are coincident in the first 30 shots. Comparing the photo taken at 0 shot with one at 30 shots, the state in the test chamber barely

changes. It indicates that the lifetimes of the bubbles contributing to the sterilization are very short. According to the pressure profile in Fig. 4, these bubbles are generated behind the concentration of the reflected shock waves because the lifetimes of cavitation bubbles are only mili-seconds according to the study of Wang and Abe [7]. From the results after the first extraction of the sample, the differences in the sterilization effect are clearly found. It suggests that the lifetimes of the generated bubbles increase so that a number of the bubbles are still remaining at least after 5 seconds. As shown in photo taken at 60 shots, the test chamber is full of these remaining bubbles. These bubbles are suggested not to be cavitation bubbles generated behind the reflected shock waves. Given those experimental situations, it is assumed that these bubbles are produced by other causes.

3.2 Role of Bubble in Shock Sterilization

Based on the results in Figs. 6, 7, and 8, there is no remarkable effect of the sterilization before the first sample extraction. The discrepancy in the experimental conditions with the extractions of the samples is concerned with the level of the liquid surface in the slot. During the experiments, only 0.1 ml of the cell suspension was regularly taken from the test chamber for the sample extraction. Although the volume of the extracted samples can be negligible comparing with the total volume of the cell suspension, the level of the liquid surface in the slot gradually decreased. Furthermore, a rapid up-and-down movement of the liquid surface in the slot was found continuously with the triggers of the electric discharges by the observation of the video camera. Figure 9 shows the sequential photos after triggering an electric discharge of 31.6 kV and 1 Hz. The initial level of the liquid surface in the slot is set to 10 mm from the upper end, that is the average of six extractions of the samples in Fig. 6. There is halation in Fig.9 (1) by the discharge flash. At 33.3 ms, the liquid surface is sloshing in the slot, the air simultaneously goes into the cell suspension, and tremendous fine bubbles are being formed in the test chamber. Bubbles moving downwards are observed as white cloud, and the test chamber is gradually filled with the generated bubbles. Hence, the remaining bubbles leading to an effective sterilization are produced in this way. It is assumed that the movement of the liquid surface in the slot is caused by the oscillation of the silicone-film separator between the two chambers. The oscillation is induced by the motion of a vapor bubble produced at the electrodes as a result of an underwater electric discharge. To confirm the generation mechanism of the bubbles, the separators of different materials and thicknesses were also used in the experiments.

Other bio-experiments were also carried out to examine the sterilization effect of these remaining bubbles. Figure 10 exhibits the change of viable cell number in time when keeping an initial liquid surface of 10 mm in the slot of the test chamber using an electric discharge of 31.6 kV and 1 Hz. The photos were obtained under the same conditions. During the experiments, the liquid surface was maintained at a fixed level by putting equivalent artificial seawater into the cell suspension after every sample extraction. The effect of the artificial seawater on the dilution of the cell suspension was considered when the sterilization effects were estimated. In the figure, the initial concentration of marine bacteria is about 6.7×10^4 cfu/ml. The number of viable cells is decreasing exponentially and all of marine bacteria are killed in about 70 seconds. It indicates the strength of the collapsing bubbles is constant and hence the number density of the generated bubbles hardly changes with the extractions of the samples, as indicated by the white area in photos. The water chamber is immediately filled with the cloud of the bubbles just after the start of the electric discharge. Figure 10 shows the sterilization effect is higher than the results in Fig. 6. On the other hand, the bio-experiments with a constant level of the liquid surface were carried out using different frequencies of the electric discharges, as same as that in Fig. 8. The results show that the sterilization effects are almost the same in all three cases. It suggests that the lifetimes of the remaining bubbles are at least 10 seconds. Comparing with the results in Fig. 8, it can be seen that effective sterilization requires a high frequency of collapsing bubbles induced by shock pressure, however, this also depends on the lifetime of the generated bubbles.

Figure 11 shows the bio-experimental results obtained by different electric discharges from 35.1 kV to 18.8 kV. The other experimental conditions were the same as that in Fig. 7. In this figure, all of the curves are found to be decreasing exponentially. Marine bacteria are killed completely in about 60 seconds with 35.1 kV, and about 180 seconds with 18.8 kV, respectively. Comparing with the results in Fig. 7, it can be seen that the number density of bubbles is mainly responsible for the sterilization effect. High sterilization effects require a large number density of bubbles. However, in fact, the bubble cloud probably prevents the incident shock wave from propagating in the water chamber in the case of an excessively large number, so that the sterilization effect could be decreased.

3.3 Role of Shock Wave in Shock Sterilization

To forcibly prevent incident underwater shock waves propagating into the test chamber, an air gap was applied between the water surface in the electric discharge chamber and the separator as shown in Fig. 12. In the experiments, a 0.1-mm silicone film, a 0.1-mm aluminum film, and a 1-mm aluminum plate were used as separators. Given the properties of these materials, it is hard to oscillate the aluminum plate by the motion of the vapor bubble produced around the electrodes in the electric discharge chamber, but easy for the aluminum film. Furthermore, it is noted that the propagation of incident shock waves is completely blocked by the aluminum material. Figure 12

shows the bio-experimental results with and without an air gap using different separators. The level of the liquid surface in the slot was maintained at 10 mm from the upper end. The output power and applied frequency of the electric charge was 31.6 kV and 1 Hz, respectively. Open squares and solid circles represent the results obtained with a 5-mm air gap using an aluminum film as separator (condition 1) and an aluminum plate (condition 2), respectively. From the observation of the test chamber, the discrepancy is that the tremendous bubbles were generated under condition 1 and not under condition 2. However, a sterilization effect was hardly attained under condition 1, as shown in the figure. The reason is that there is no shock pressure inducing the collapse of the bubbles in the test chamber because the air gap and the separator exclude the incident shock waves. Consequently, an incident shock wave plays a vital role on the shock sterilization method.

Solid diamonds and triangles indicate the bio-experimental results using the silicone film as a separator without an air gap (condition 3) and with an air gap (condition 4). The observation of the test chamber shows that the number of the generated bubbles was almost same in both cases, but apparently larger than that under condition 1. In the figure, all of marine bacteria are killed after 70 seconds under condition 3. It should be noted that marine bacteria are also completely killed after 100 seconds under condition 4. Comparing condition 1 with condition 2, marine bacteria are not killed in the presence of bubbles alone without incident shock waves. In fact, an excellent sterilization effect is obtained under condition 4 when incident shock waves are stopped entering the test chamber by the air gap. Hence, this suggests that underwater shock waves exist in the test chamber under condition 4. To understand the behaviors of the shock waves, an optical experiment was conducted using a high-speed camera (I-SPEED 7, Nac Image Technology) combining with the pressure measurement of FOPH.

It is hard to observe the behaviors of the shock waves in the present cylindrical water chamber, so that a cuboidal water chamber as shown in Fig. 13 was prepared. The water chamber consisted of two equivalent cubic parts, i.e., an electric discharge chamber and a test chamber. The length of each part in the water chamber was 30 mm. The electrodes were equipped at a position of 20 mm from the silicone separator.

Figure 14 shows the propagation of the shock waves with a 5-mm air gap as observed using the schlieren method. A metal halide lamp (LS-M350, SUMITA Optical Glass Inc.) was used as an optical light source. The high-speed camera captured images at a frame rate of 100 kfps with an exposure time of 300 ns. The resolution of the images was 840 $\times$ 216 pixels. The other experimental conditions were the same as that in Fig. 12. In Fig. 14 (1), the incident shock waves are reflected on the water surface, the walls of both sides, and the bottom boundary, as indicated using RSW. Subsequently, similar as the part of the shock wave propagating into the bottom of the acrylic wall, the part in both sides of the acrylic wall is re-entering water in the test chamber as a compression oblique wave (SW1) as shown in the left side in the frame 2. Shock wave 2 (SW2) in the middle is the transmitted part of the incident shock wave directly through the air gap. After that, the propagations of several weak shock waves are just recognized in the test chamber as indicated by the arrows in Figs. 14 (3)-(5).

The corresponding pressure profile is shown in Fig. 15. The pressure history with the aluminum film separator is also presented in the figure as the reference data. In the referred pressure profile, it is confirmed that the noise range of the pressure transducer is about from 1 MPa to -1 MPa except the data within about 2 μs affected by the noise of the discharge flash. Comparing with the referred pressure profile, we can find that there are several shock pressures of lower than 2 MPa from 10 μs in the case of the silicone film. Based on the observation in Fig. 14, these pressures should correspond to SW1 and SW2. From the pressure variations after 50 μs, the collapses of the bubbles are expected in the test chamber. These results explain that the shock pressures inducing the bubble collapse under condition 4 in Fig. 12 are the transmitted shock waves through the air gap and the wall material. It should note that these shock waves of lower than 2 MPa give rise to such an excellent sterilization effect comparing with 6.9-MPa pressure without an air gap. Consequently, the pressure value of the incident shock wave cannot be a main factor in increasing the sterilization effect, although it plays a vital role in the shock sterilization method.

3.4 Role of Free Radicals in Shock Sterilization

The mechanism of the shock sterilization method is explained by the mechanical action of rebound shock pressure and bio-chemical action of free radicals. To attain the sterilization effects of only rebound shock waves, sodium L-ascorbate was added to get rid of the action of free radicals in the cell suspension. Figure 16 shows the estimates of the number of viable cells at 31.6-kV electric discharges with and without sodium L-ascorbate. Solid diamonds on blue curve indicate the results without sodium L-ascorbate. Marine bacteria are perfectly killed in about 70 seconds. Solid squares on red curve represent the results with sodium L-ascorbate. It is found that the number of viable cells constantly keeps throughout the experiment. Hence, we consider that there were no direct

mechanical effects from the bubble motion on killing marine bacteria in the cylindrical water chamber, i.e., the free radicals produced with the bubble motion are mainly responsible for the inactivation of marine bacteria.

In the previous research, Abe et al. [12] used a gas gun to investigate the tolerance of marine *Vibrio* sp. against the shock pressure. They found that these viable cells were completely inactivated by a 200-MPa shock wave when sodium L-ascorbate was used in experiments. Furthermore, they also reported that a strong pressure pulse of 200 MPa was maintained for about 20 μs after the interaction of microbubbles with a shock pressure generated by explosives of a 10-mg AgN_3 [14]. There results suggest that the mechanical action of rebound shock wave generated by the microbubble collapse is potentially capable of killing marine *Vibrio* sp.. The reason for no sterilizing action in Fig. 16 is that strong rebound shock waves are not generated in the cylindrical water chamber. The theoretical solutions to the Herring equation reported by Wang and Abe [13] suggests that the strength of rebound shock wave depends on the bubble size for a given pressure profile of incident shock wave. The bubbles with diameters of around 30 μm probably produce much stronger rebound shock waves to kill marine bacteria for the pressure profile in Fig. 4. Therefore, rebound shock waves cannot contribute effectively to the sterilization when the size of the generated bubbles becomes larger or the pressures of the incident shock waves are lower in the cylindrical water chamber.

Chemical radicals that have a close relationship with killing marine bacteria are released at the minimum size during collapsing process of bubbles because extreme high temperature and pressure inside a bubble destroy chemical bonds of vapor molecules and non-condensable gases (including air). Hydroxyl (OH) radicals are dominant radical species with extreme high oxidization [15]. However, it is difficult to measure directly their generation because of their high and fast actions in a dynamic stimulus. Therefore, we measured one of the products of their chemical reactions, H_2O_2, to confirm quantitatively the presence of the OH radicals [16]. A digital pack tester (DPM-H2O2, Kyoritsu Chemical-Check Lab., Corp.) that relies on 4-Amino-antipyrine spectrophotometric method was used to measure the H_2O_2 concentration. Its measuring range is from 0.10 to 2.0 mg/ L and the resolution is 0.05 mg/L. External dimension of the digital pack tester as shown in Fig. 17 is 145 mm (L) ×68 mm (W) ×48 mm (H). The figure also shows the results of the concentration of the H_2O_2 in the cylindrical test chamber filled with the distilled water and the artificial seawater after the electric discharges of 3000, 5400, and 7200 shots were carried out with 31.6-kV and 1 Hz. The symbols in the figure indicate of the averages for 5-set measurements that are all the same due to the respectively small resolution of the digital pack tester. It is found that the concentration of the H_2O_2 increases with the number of the electric discharges. Furthermore, the concentration of the H_2O_2 in the artificial seawater is larger than that in the distilled water. Such different results of the concentrations in respective waters are thought to be caused by the bubble size and the number density of bubbles. Smaller size and larger number density of the bubbles are produced in artificial seawater due to their small surface tension. Therefore, the strength of the bubble collapse in artificial seawater is stronger than that in distilled water, so that the products of the OH radicals in artificial seawater are considered to be larger.

According to the results in Fig. 16, the action of free radicals is mainly responsible for killing marine bacteria under condition 4 of the silicone film with an air gap shown in Fig. 12. Here, the shock pressure in the test chamber probably become very low, but a high sterilization effect was obtained. To estimate free radical generation by the interaction of such a weak shock wave with a small bubble, the bubble motion is analyzed by solving the Herring Equation [17]. In the theoretical analysis, it is assumed that the bubble is filled with the ideal gas, air, according to the generation mechanism of the bubbles inducing effective sterilization. Consequently, we neglect the non-equilibrium evaporation and condensation of water vapor, i.e., the mass exchange at the interface [18]. Because of temperature variation during the bubble motion, it requires to take into account the thermal conduction between the bubble interior and the surround liquid. Dularand and Coutierdelgosha [19] argued that the thermal transfer occurs within a thermal boundary layer in the liquid around the bubble. The thickness of the boundary layer can be estimated using the thermal diffusivity and the Rayleigh-Plesset collapse time [20]. Subsequently, the Fourier law is used to investigate the heat released from the bubble to the liquid through the layer. Finally, the equation of state for ideal gas is applied to determination of the temperature and pressure inside the bubble. The corresponding equations are presented in the Appendix.

Figure 18 shows the theoretical solution of a 0.1-mm diameter bubble exposed to a planar shock pressure of 0.1 MPa to 7 MPa. The pressures of 2 MPa and 6.9 MPa are obtained from the experiments as average values with and without an air gap at an electric discharge of 31.6 kV, respectively. The initial diameter of the bubble took about 0.1 mm based on the optical images. Figure 18 (a) and (b) present the variations of the ratio of the minimum to the initial bubble radius and the corresponding maximum pressure and temperature inside the bubble with the exposed pressure, respectively. In Fig. 18 (a), it is found that a bubble contracts to smaller radius with an increase of the exposed pressure. The maximum temperature and pressure increase correspondingly, and in the case of a 6.9-MPa exposed pressure they reach respective values, 1938 K and 4870 MPa. For a 2-MPa of shock pressure, when a

bubble contracts to 0.093-time initial radius, the maximum temperature and pressure inside the bubble reach about 1087 K and 474 MPa, respectively.

In other researches, Locke et al. [21] used a planar laser-induced fluorescence method to investigate a large-scale and high-pressure combustor environment and obtained the images of the OH radicals at the inlet of 1034 kPa and 866 K. Varatharajan and Williams [22] investigated the high-temperature oxidation of acetylene numerically and theoretically, and reported that the OH radicals were formed by the reaction of the H radicals and O_2 under the initial condition of 50 bar and 1100 K. The density of the OH radicals was also measured using a laser induced fluorescence in homogeneous pressure plasmas of 460 MPa in the study of Magne et al. [23] when they used a photo-triggered discharge to investigate the production kinetic mechanism and reactivity of the OH radical in a N2/O2 mixture. The study by Abe et al. [12] also indicated free radicals could be generated after the passage of underwater shock waves with amplitude of about 200 MPa at 293 K. From the above-mentioned work, the OH radicals are produced when bubbles interact with a shock pressure of 2 MPa under condition 4 in Fig. 12 or even much lower. Comparing with the formation of strong rebound shock wave, for the condition to produce free radicals by the bubble-shock wave interaction, it is not necessary to expose smaller bubble than 50 μm to a high pressure of incident shock wave. Hence, improvement of the sterilization effect is much more easily realized by increasing the action of free radicals than rebound shock wave.

4. Conclusions

The paper reported on a fundamental study to investigate sterilization effects in a cylindrical water chamber with supply of only underwater shock waves. Bio-experiments of marine *Vibrio* sp. were carried out under different strength and frequencies of the incident shock waves generated by a high-voltage power supply. To prevent the production of the electric discharges from entering the cell suspension, a silicone film was used to separate the two chambers. According to the experimental pressure profile, the incident shock waves were reflected on the inner wall and then concentrated in the central axis of the water chamber. Cavitation bubbles were probably generated due to the expansion regions behind the concentration of the reflected shock waves. From the results of the bio-experiments, all of marine bacteria were killed in a short time, and the sterilization effects increased with the strength and frequency of the bubble collapse. However, it also depended on the lifetime of bubble. Combining with the observation of the states in the test chamber, it was found that a rapid up-and-down movement of the liquid surface in the slot mainly produced numerous fine bubbles due to rapid motion of a vapor bubble at the electrodes. These results show that an excellent sterilization effect requires a large number density of bubbles.

The role of shock wave in the shock sterilization was investigated with an air gap to prevent incident underwater shock wave propagating into the test chamber with different separators. A sterilization effect was hardly represented by only tremendous bubbles without a shock pressure. In addition, note that a high sterilization effect was even obtained with an air gap. The schlieren observation showed that very weak shock waves passed through the air gap and the wall material, and entered the test chamber. Consequently, the collapses of the bubbles were caused by these weak shock waves. These results showed that it is not necessary to expose micron-sized bubbles to strong shock pressures for an effective sterilization.

Finally, the results of the bio-experiments with sodium L-ascorbate exhibited that, free radicals produced with the adiabatic compression of the bubbles contributed mainly to killing marine bacteria in the present water chamber, and it was thought that the direct mechanical effect of the bubble motion were not responsible effectively owing to large size of the bubbles and low pressure of the incident shock waves. The generation of the OH radicals was clarified by measuring the concentration of H_2O_2. Its concentration in artificial seawater was larger than that in distilled water because much smaller size and a larger number of bubbles were generated in artificial seawater. The theoretical solution to the Herring equation showed that improvement of sterilization effect was much more easily realized by increasing the action of free radicals using the collapsing motion of bubble. Finally, it is proven that a high-effect sterilization is reached with supply of only underwater shock wave of tens of atmosphere based on a bubble-shock wave interaction.

Acknowledgement

This work was supported by the JSPS KAKENHI, grant Numbers 16H04600 and 16K14512, and the National Natural Science Foundation of China, grant numbers 11772340 and 11332011. In addition, we would like to sincerely thank Nac Image Technology Inc. for the supply of optical experimental equipment.

Appendix

The Herring bubble equation is applied considering the compressibility of water when the speed of sound is assumed to be constant, as shown in Eq. (1),

$$\left(1-\frac{2\dot{R}}{C_\infty}\right)R\ddot{R}+\frac{3}{2}\left(1-\frac{4}{3}\frac{\dot{R}}{C_\infty}\right)\dot{R}^2+\frac{1}{\rho_\infty}\left(P_\infty-P_s-\frac{R}{C_\infty}\frac{dP_s}{dt}\right)=0, \quad (1)$$

where R is the bubble radius, $\dot{R}$ = dR/dt, t is the time, $\ddot{R}$ = d$\dot{R}$ /dt. C_∞ is the sound speed of water at infinity, ρ_∞ is the density of water at infinity, and P_s is the pressure at the wall of a bubble. P_∞ is the external pressure behind the induced shock wave.

C_∞ is given by

$$C_\infty=\sqrt{\frac{n(P_\infty+B)}{\rho_\infty}}, \quad (2)$$

where B and n are constant values, B = 2963 bar and n = 7.41.

P_s is described by

$$P_s=P_{in}-\frac{1}{R}\left(2\sigma+4\mu\dot{R}\right), \quad (3)$$

where σ is the surface tension, and μ is the viscosity coefficient, and P_{in} is the pressure of the gas inside the bubble, as shown in Eq. (4),

$$P_{in}v=R_gT_{in}. \quad (4)$$

where v and T_{in} is the molar volume and temperature of the gas inside the bubble, and R_g = 8.3145 J/(mol K).

When considering the effect of the thermal conduction at the bubble wall, the energy balance of the gas inside the bubble is written in Eq. (5) based on the study by Dularand and Coutierdelgosha [19], where the bubble radius varies from R to R+ΔR and the gas temperature changes by ΔT during the time Δt:

$$\left(\frac{4}{3}\pi R^3\right)\rho_g C_{vg}\Delta T=-(\Delta Q+P_s(4\pi R^2\Delta R)) \quad (5)$$

where ρ_g is the gas density and varies with the temperature and pressure inside the bubble, C_{vg} is the specific heat of gas at constant volume. The term on the left-hand side presents the variation of the internal energy of the gas during the time Δt, the second term on the right-hand side is the work of the pressure force at the bubble surface, and ΔQ is the heat released from the bubble to the liquid.

Dularand and Coutierdelgosha [19] argued that the thermal exchange occurs within a thermal boundary layer in the liquid around the bubble. Hence, ΔQ can be written in Eq. (6) according to the Fourier's law,

$$\Delta Q\approx\frac{\lambda_l(4\pi R^2)\Delta T}{\delta}\Delta t=\frac{\lambda_l(4\pi R^2)(T_{in}-T_0)}{\delta}\Delta t. \quad (6)$$

where δ is the thickness of the thermal boundary layer, λ_l is the thermal conductivity, T_0 and T_{in} are the temperature of the gas inside the bubble at t = 0 and t + Δt.

Franc et al. [20] proposed that the thickness δ of the thermal boundary layer is of the order of $\sqrt{\alpha_l l/V}$, with α_l the thermal diffusivity in the liquid, l the length of the cavity, and V the flow velocity. In the present study, the thickness δ is estimated using the Rayleigh-Plesset collapse time τ_c.

$$\delta=\sqrt{\alpha_l\tau_c}=\sqrt{a_l 0.915R_0\sqrt{\frac{\rho_l}{p_\infty-P_0}}}=\sqrt{(\lambda_l/\rho_l c_{pl})0.915R_0\sqrt{\frac{\rho_l}{p_\infty-P_0}}} \quad (6)$$

where C_{pl} and ρ_l the heat capacity at constant pressure and the density in the liquid, and P_0 is the atmospheric pressure.

Finally, Herring bubble equation are solved using the fourth-order accurate Runge-kutta-Gill method. In this analysis, the density of water ρ_∞ = ρ_l = 999.7 kg/m^3, the viscosity coefficient μ = 1.307 $\times 10^{-3}$ Pa·s, the surface tension σ = 74 $\times$ 10^{-3} N/m, the density of gas ρ_g = 1.20 kg/m^3 at T_0 = 293.15 K when R = R_0 , the specific heat of

gas C_g = 1012 J/(kg·K), the thermal conductivity in the liquid λ_l =0.599 W/(m·K), the heat capacity C_{pl} = 4186 J/(kg·K) , the atmospheric pressure P_0 =1.01325 $\times 10^5$ Pa were used.

Reference

[1] K. Takayama, Application of Underwater Shock Wave Focusing to the Development of Extracorporeal Shock Wave Lithotripsy, Japanese Journal of Applied Physics 32 (1993) 2192-2198.

[2] K. Hokamoto, M. Fujita, H.Shimokawa, H. Okugawa, A new method for explosive welding of Al/ZrO 2 joint using regulated underwater shock wave, Journal of Materials Processing Technology 85 (1999) 175-179.

[3] A. M. Loske, U. M. Alvarez, C. Hernández-Galicia, E. Castaño-Tostado, F. E. Prieto, "Bactericidal effect of underwater shock waves on Escherichia coli ATCC 10536 suspensions, Innovative Food Science & Emerging Technologies 3 (2002) 321-327.

[4] A. Abe, H. Mimura, H. Ishida, K. Yoshida, The effect of shock pressures on the inactivation of a marine *Vibrio* sp, Shock Waves 17 (2007) 143-151.

[5] M. Takahashi, K. Chiba, P. Li, Free-radical generation from collapsing microbubbles in the absence of a dynamic stimulus., The Journal of Physical Chemistry B 111 (2007) 1343-1347.

[6] L. Beneš, Z. Ďuračková, M. Ferenčik, Chemistry, physiology and pathology of free radicals, Life sciences, 65 (1999) 1865-1874.

[7] J. Wang, A. Abe, Experimental Verification of Shock Sterilization for Marine *Vibrio* sp. using Microbubbles Interacting with Underwater Shock Waves, Journal of Marine Science and Technology 21 (2016) 679-688.

[8] J. Wang, A. Abe, T. Koita, M. Sun, Contribution of Cavitation Generation to Shock Wave Sterilization Effects in a Narrow Water Chamber, The proceeding of 31th International Symposium on Shock Waves, in press (2017)

[9] M. Delius, F. Ueberle, W. Eisenmenger, Extracorporeal shock waves act by shock wave-gas bubble interaction, Ultrasound in medicine & biology 24 (1998) 1055-1059.

[10] M. Lokhandwalla, B. Sturtevant, Mechanical haemolysis in shock wave lithotripsy (SWL): I. Analysis of cell deformation due to SWL flow-fields, Physics in medicine and biology 46 (2001) 413-437.

[11] J. Sundaram, B. R. Mellein, S. Mitragotri, An experimental and theoretical analysis of ultrasound-induced permeabilization of cell membranes, Biophysical journal 84(2003) 3087-3101.

[12] A. Abe, H. Mimura, Sterilization of Ships' Ballast Water, Bubble Dynamics and Shock Waves, Springer Berlin Heidelberg (2013) 339-362.

[13] J. Wang, A. Abe, A hybrid analytical model of sterilization effect on marine bacteria using microbubbles interacting with shock wave, Journal of Marine Science and Technology 21 (2016) 385-395.

[14] A. Abe, K.Ohtani, K. Takayama, S. Nishio, H. Mimura, M. Takeda, Pressure generation from micro-bubble collapse at shock wave loading, Journal of Fluid Science and Technology 5 (2010) 235-246.

[15] T. G. Leighton, The Acoustic Bubble, Academic Press: London (1994).

[16] K. Kanthale, M. Ashokkumar, F. Crieser, Sonolumimescence, sonochemisty (H_2O_2) and bubble dynamics: Frequecy and power effects, Ultrasonics Sonochemisty 15 (2008) 143-150.

[17] C. Herring, Theory of the pulsations of the gas bubble produced by an underwater explosion, Columbia Univ., Division of National Defense Research (1941).

[18] K. Yasui and K. Kato, Bubble dynamics and sonoluminescence from helium or xenon in mercury and water, Physical Review E Statistical Nonlinear & Soft Matter Physics 86 (2012) 036320.

[19] M. Dularand, O. Coutierdelgosha, Thermodynamic effects during growth and collapse of a single cavitation bubble, Journal of Fluid Mechanics 736 (2013) 44-66.

[20] J. Franc, C. Rebattet, A. Coulon, An Experimental Investigation of Thermal Effects in a Cavitating Inducer, Jundishapur Journal of Natural Pharmaceutical Products 126 (2004) 716-723.

[21] R.J. Locke, K.A. Ockunzzi, OH Imaging In a Lean Burning High-Pressure Combustor, AIAA Journal 34 (1996) 622-624.

[22] B. Varatharajan, F.A. Williams, Chemical-Kinetic Descriptions of High-Temperature Ignition and Detonation of Acetylene-Oxygen-Diluent System, Combustion &Flame 124 (2001) 624-645.

[23] L. Magne, S. Pasquiers, N. Bilin-Simiand, C. Postel, Production and reactivity of the hydroxyl radical in homogeneous high pressure plasmas of atmospheric gases containing tracers of light olefins, Journal of Physics D: Applied Physics 40 (2007) 3112-3127.

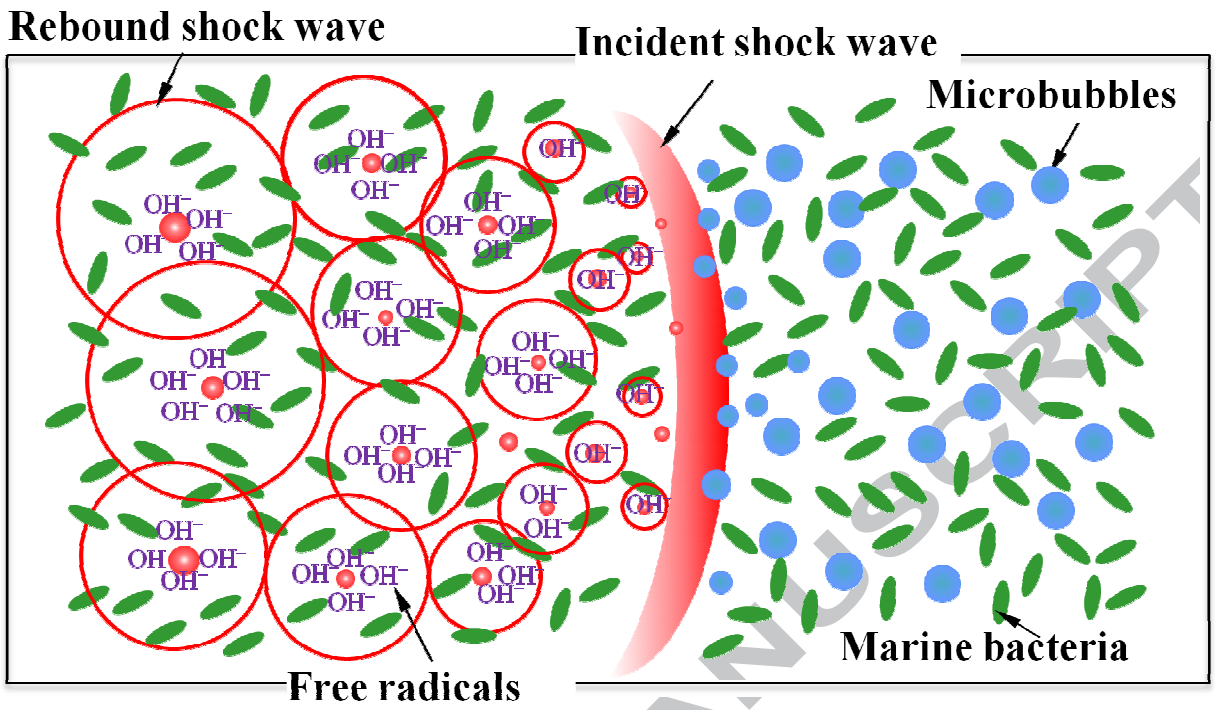

Fig. 1

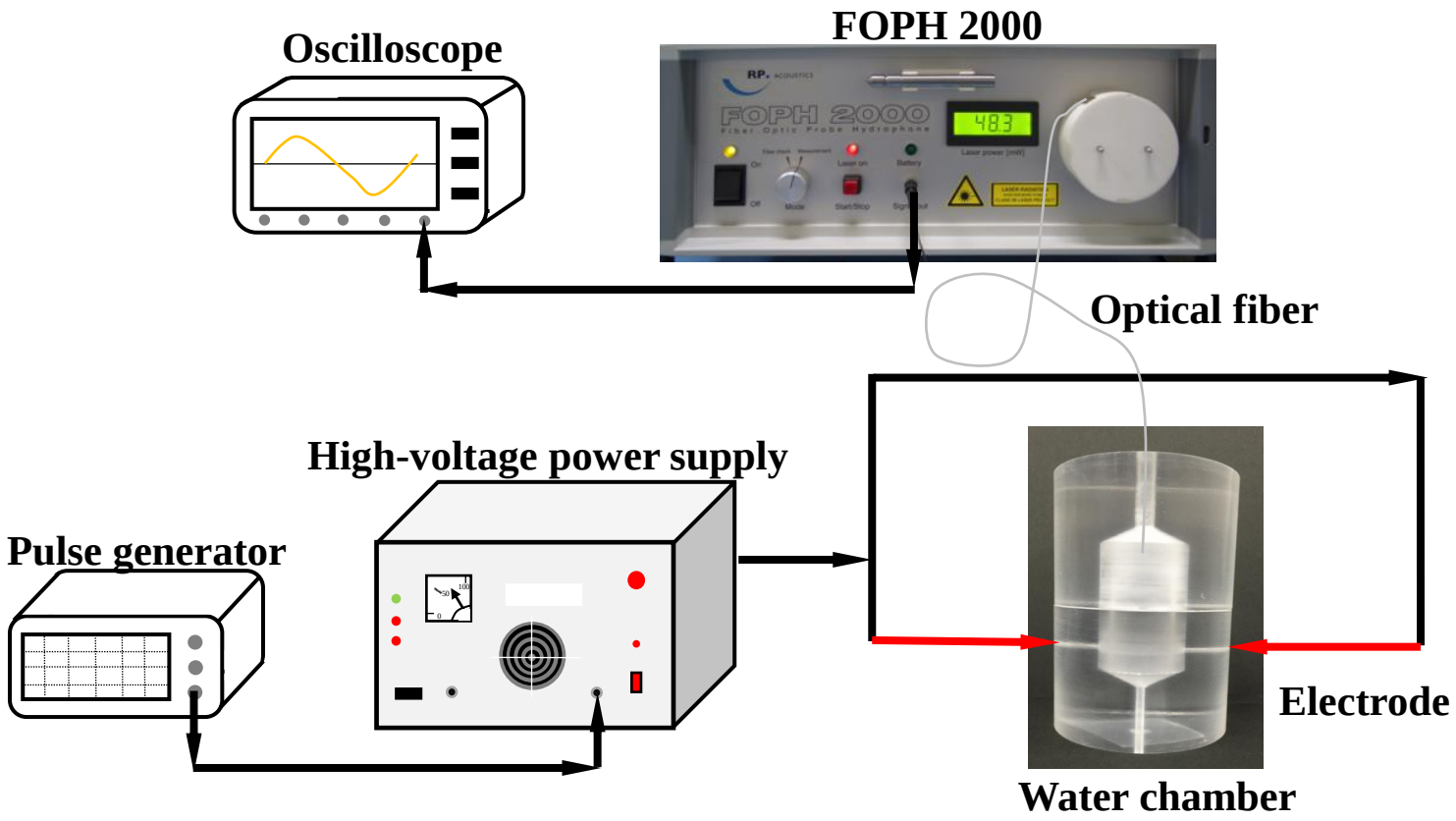
Oscilloscope
FOPH 2000
FOPH 2000
Optical fiber
High-voltage power supply
Pulse generator
Electrode
Water chamber

Fig. 2

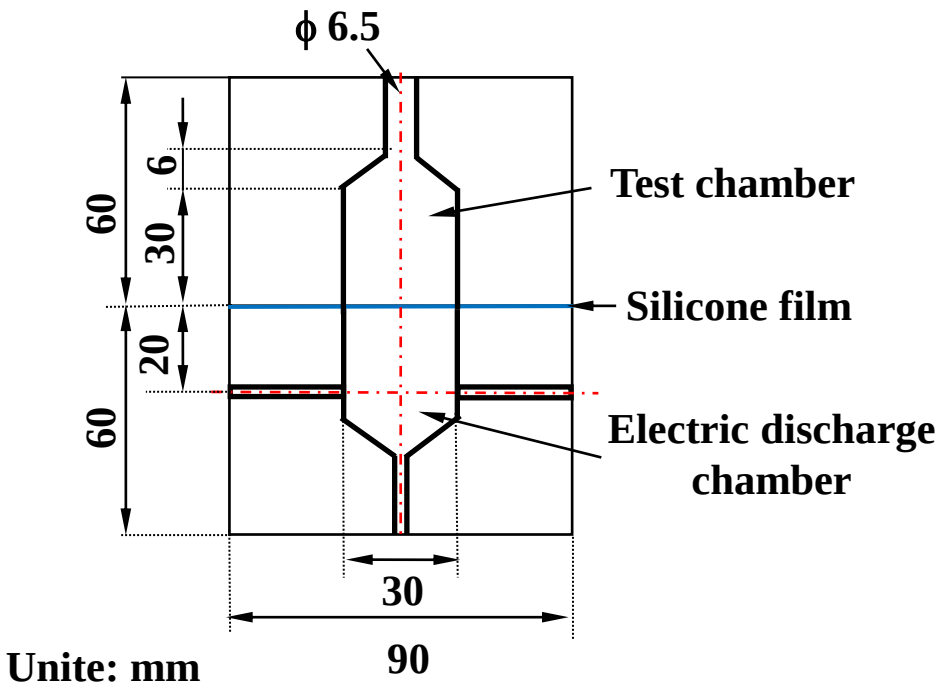
ϕ 6.5
60
6
30
20
60
Test chamber
Silicone film
Electric discharge chamber
30
90
Unite: mm

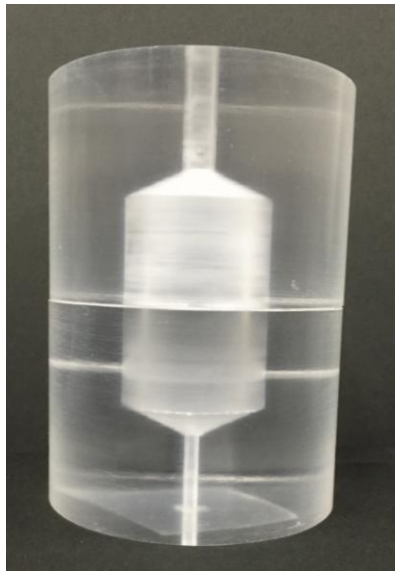

Fig. 3

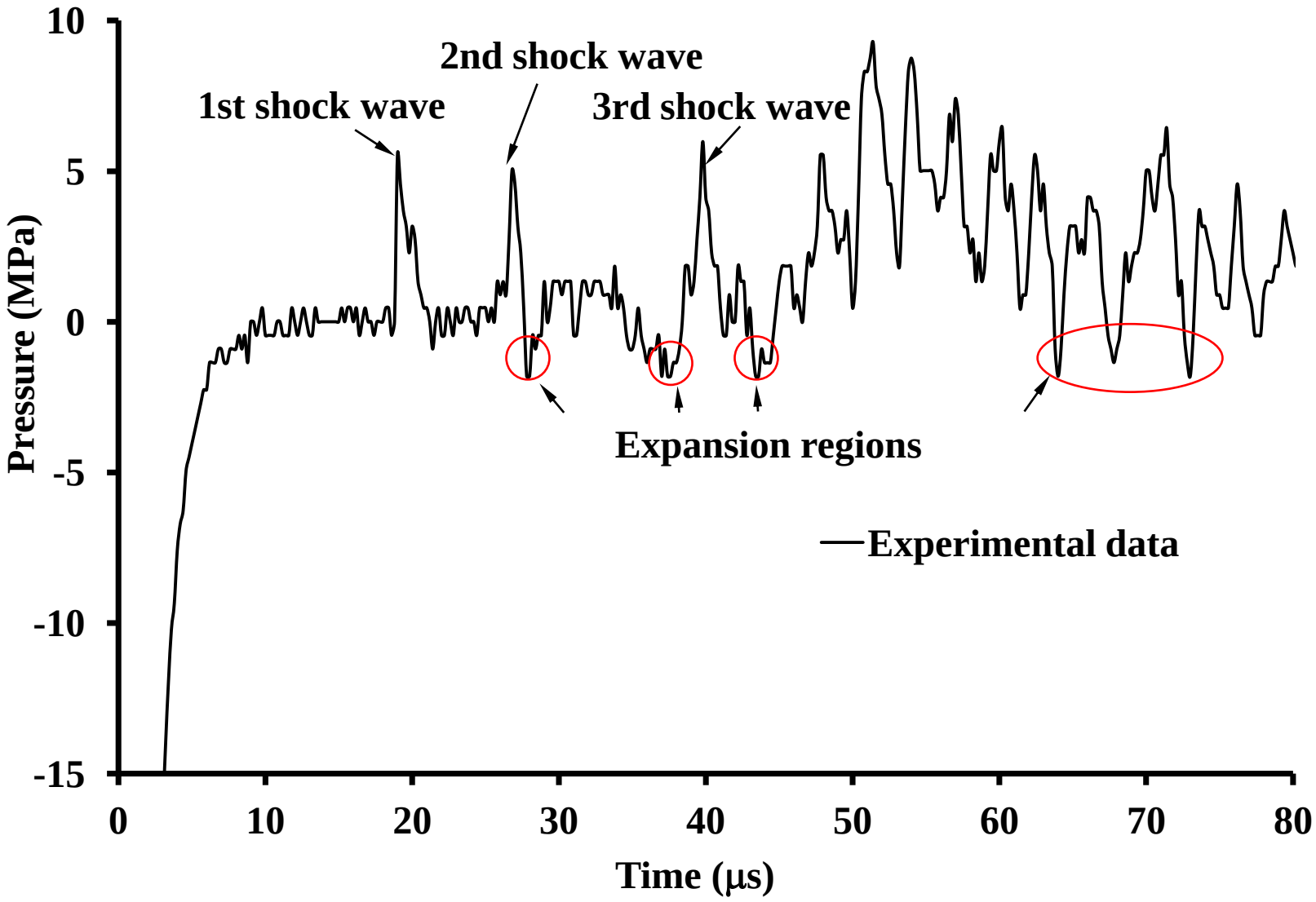
10
5
0
-5
-10
-15
Pressure (MPa)
0
10
20
30
40
50
60
70
80
Time (μs)
1st shock wave
2nd shock wave
3rd shock wave
Expansion regions
Experimental data

Fig. 4

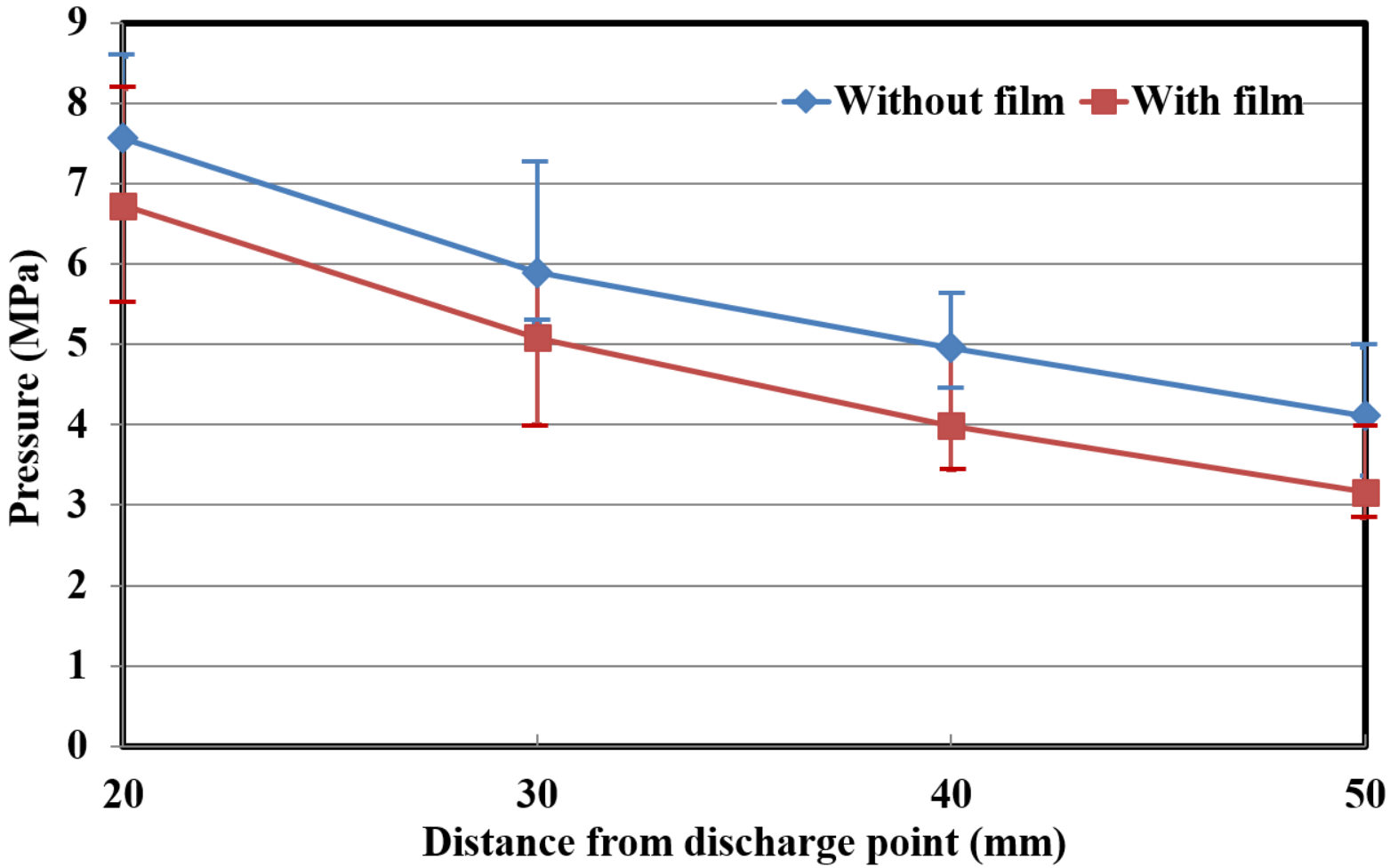
Without film
With film
Pressure (MPa)
0
1
2
3
4
5
6
7
8
9
20
30
40
50
Distance from discharge point (mm)

Fig. 5

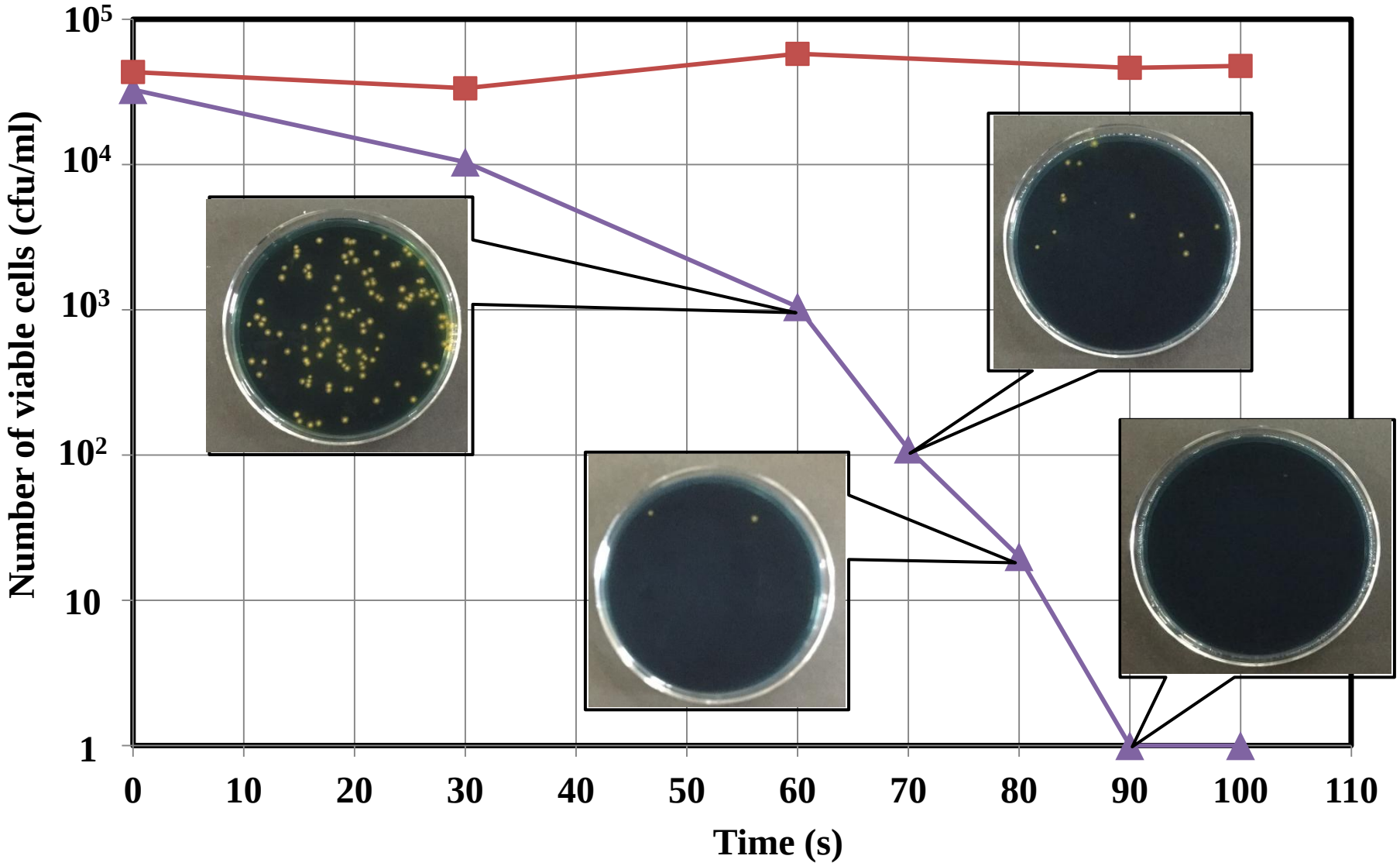
Number of viable cells (cfu/ml)
10^5
10^4
10^3
10^2
10
1
0
10
20
30
40
50
60
70
80
90
100
110
Time (s)

Fig. 6

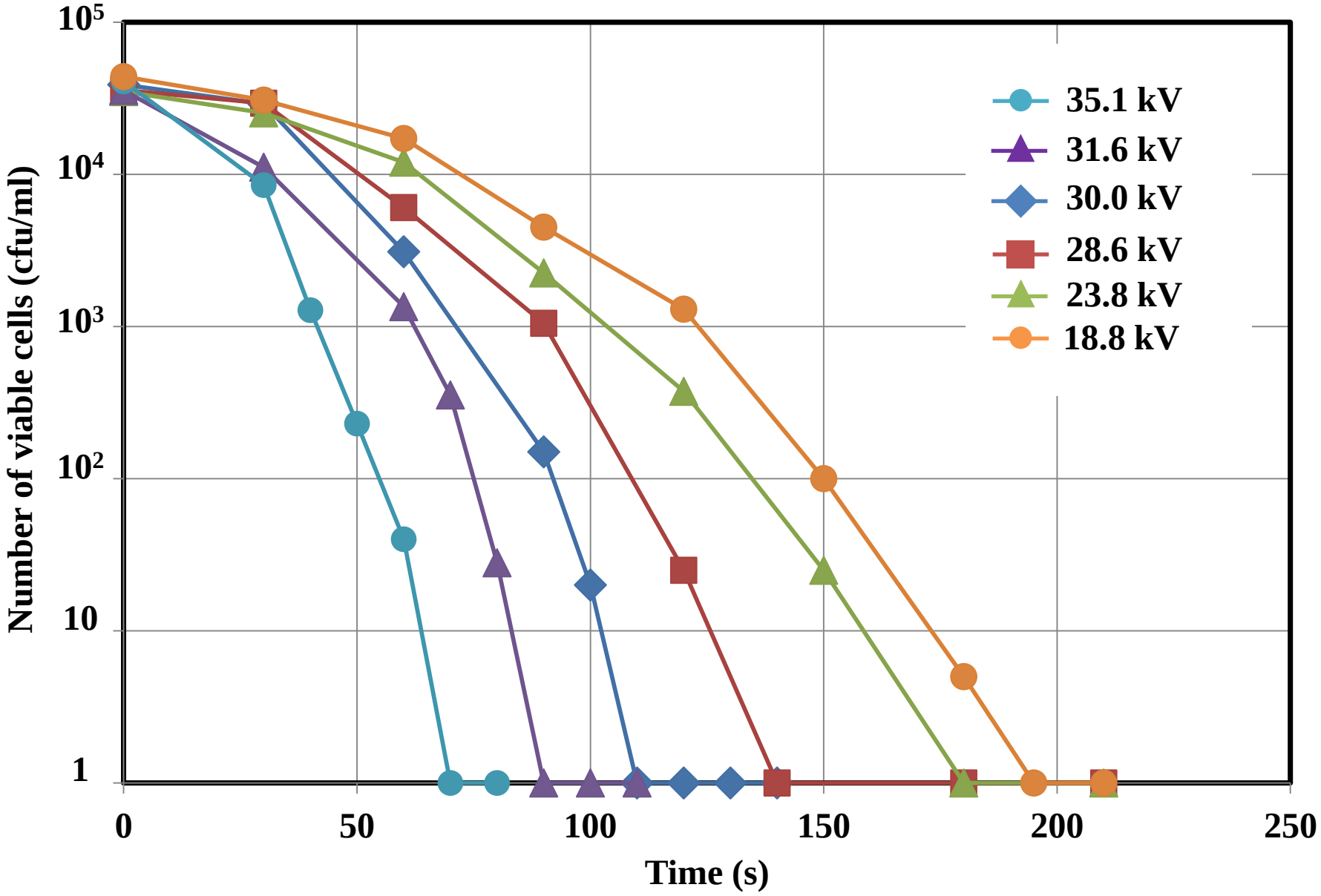
Number of viable cells (cfu/ml)
10^5
10^4
10^3
10^2
10
1
0
50
100
150
200
250
Time (s)
35.1 kV
31.6 kV
30.0 kV
28.6 kV
23.8 kV
18.8 kV

Fig. 7

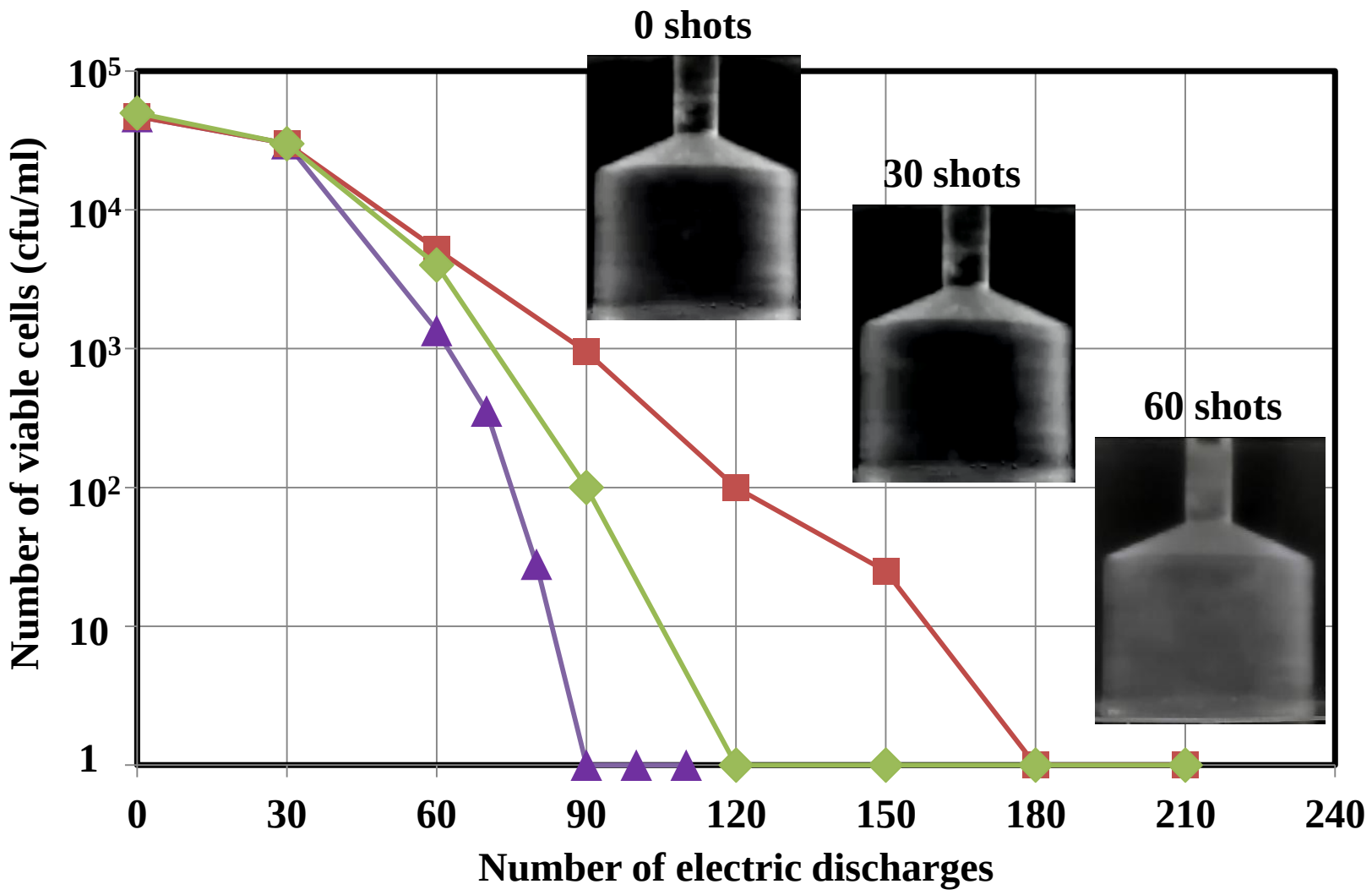
0 shots
30 shots
60 shots
Number of viable cells (cfu/ml)
10^5
10^4
10^3
10^2
10
1
0
30
60
90
120
150
180
210
240
Number of electric discharges

Fig. 8

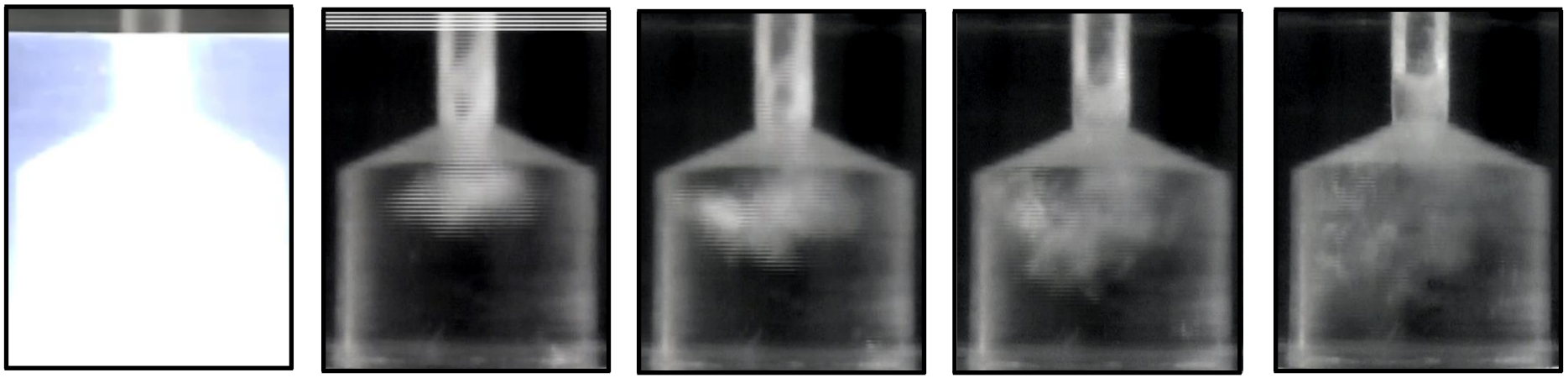

(1) 0 ms (2) 33.3 ms (3) 66.7 ms (4) 100 ms (5) 133.3 ms

Fig. 9

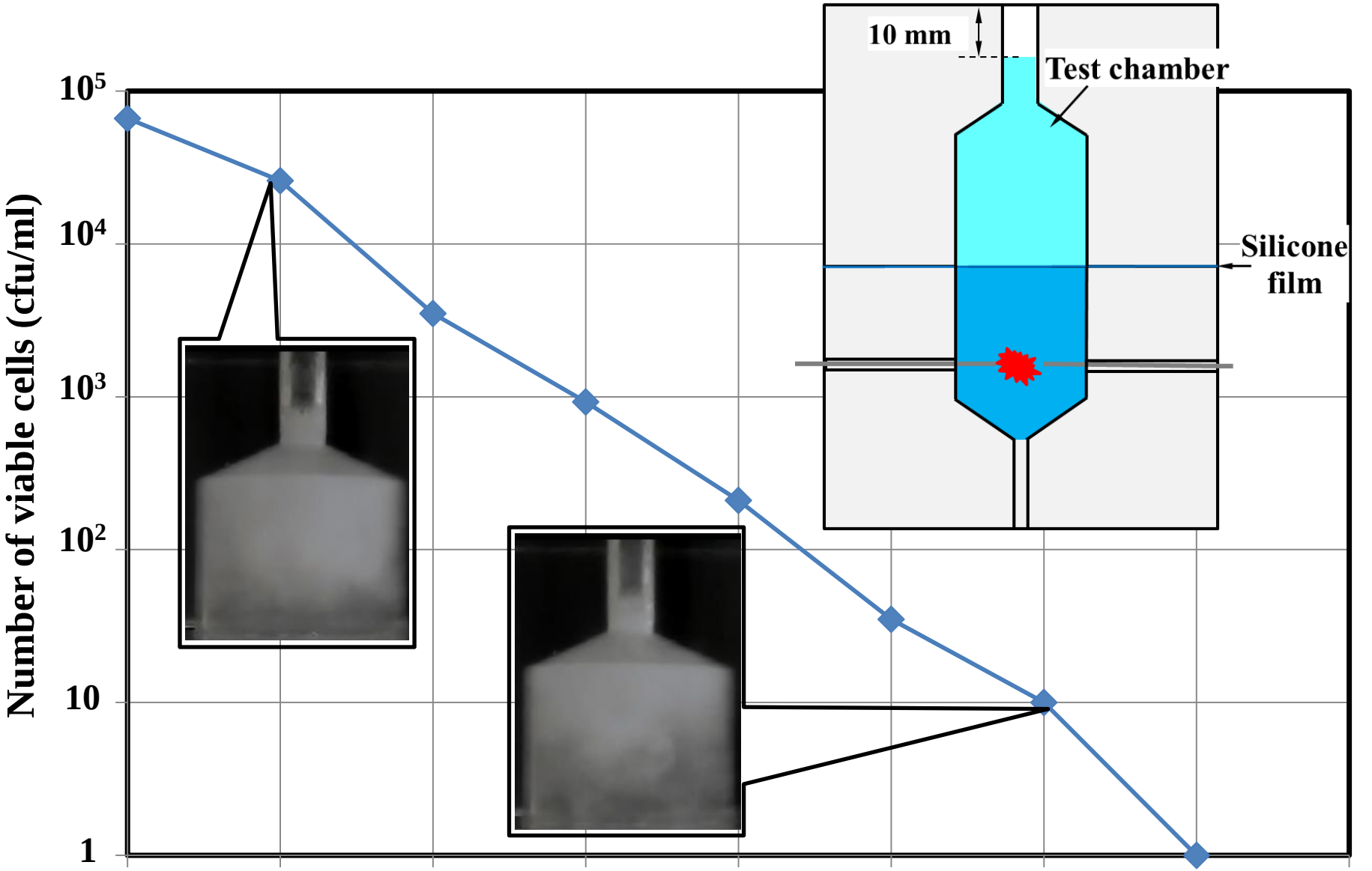
10 mm
Test chamber
Silicone film
Number of viable cells (cfu/ml)
10^5
10^4
10^3
10^2
10
1
0
10
20
30
40
50
60
70
80
Time (s)

Fig. 10

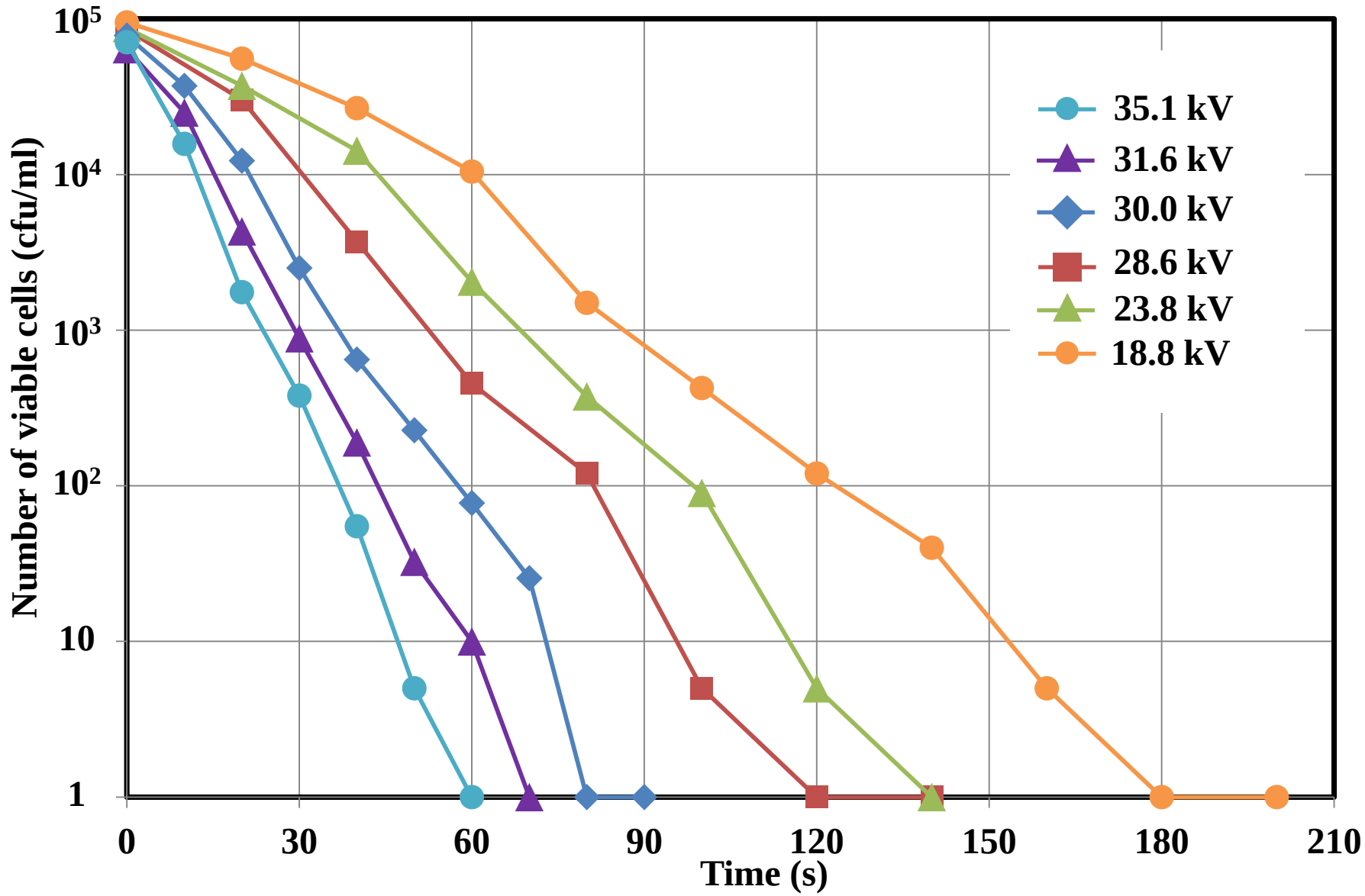
Number of viable cells (cfu/ml)
10^5
10^4
10^3
10^2
10
1
0
30
60
90
120
150
180
210
Time (s)
35.1 kV
31.6 kV
30.0 kV
28.6 kV
23.8 kV
18.8 kV

Fig. 11

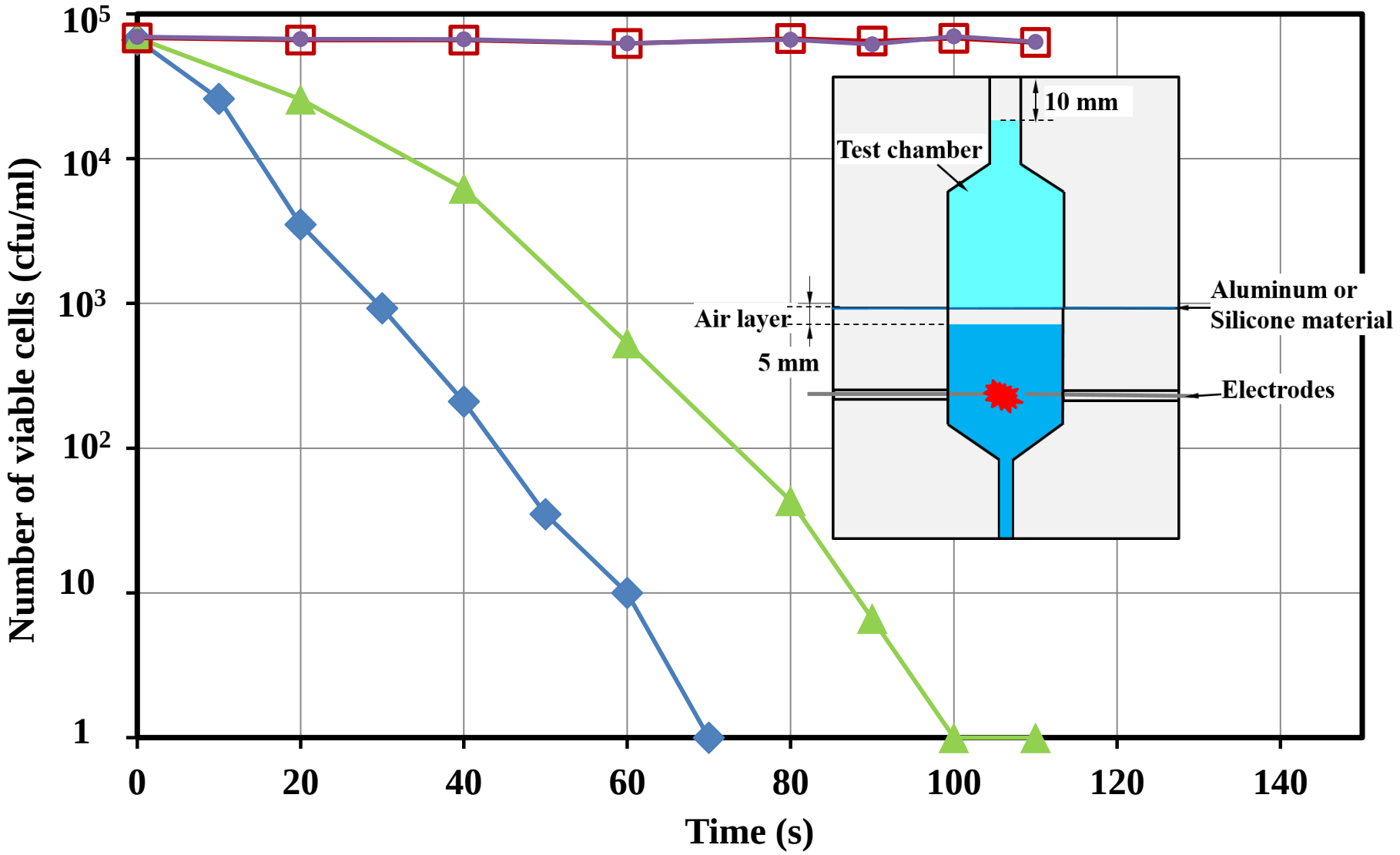
Number of viable cells (cfu/ml)
10^5
10^4
10^3
10^2
10
1
0
20
40
60
80
100
120
140
Time (s)
10 mm
Test chamber
Air layer
5 mm
Aluminum or
Silicone material
Electrodes

Fig. 12

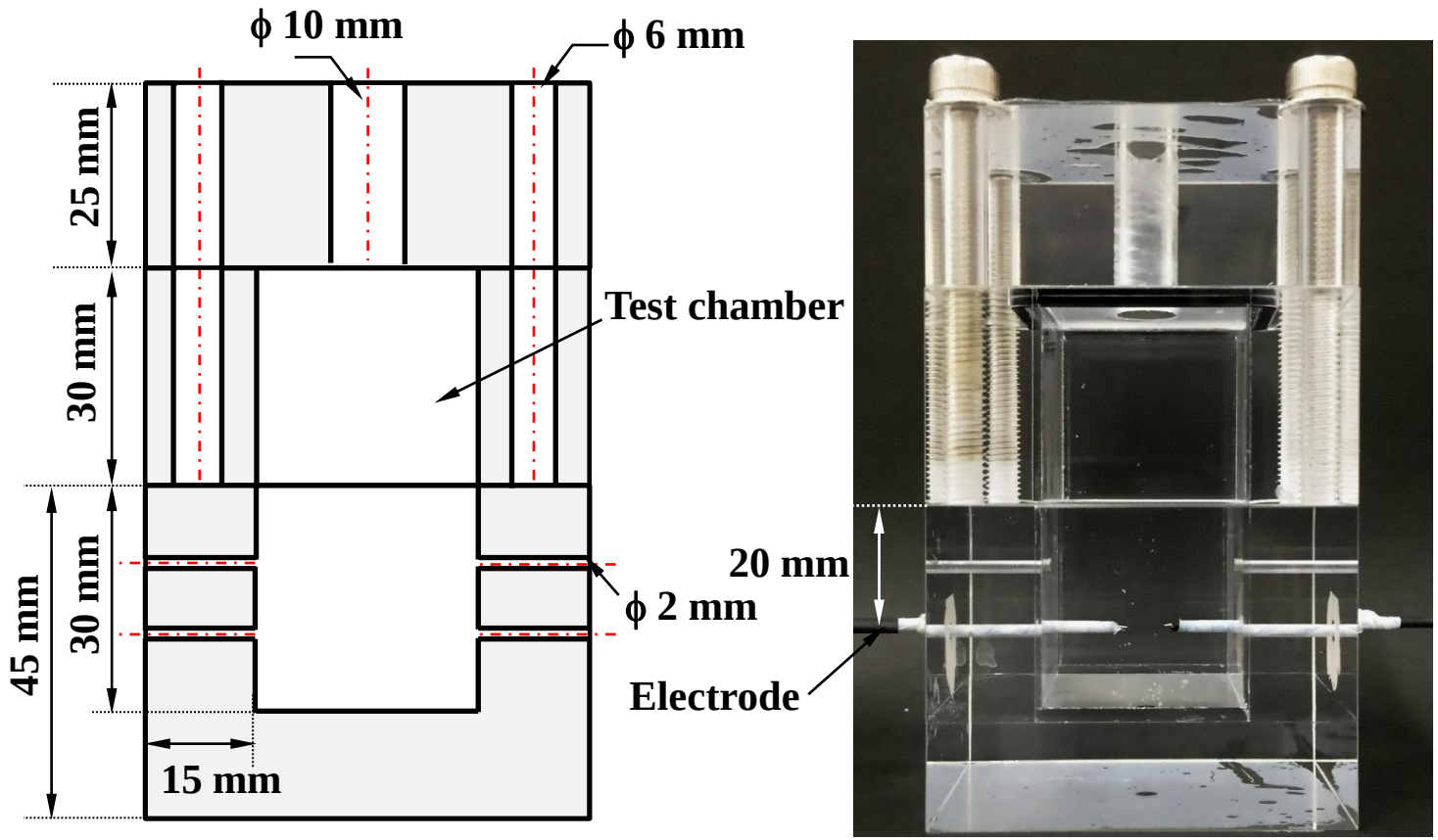
ϕ 10 mm
ϕ 6 mm
25 mm
30 mm
Test chamber
45 mm
30 mm
ϕ 2 mm
15 mm
20 mm
Electrode

Fig. 13

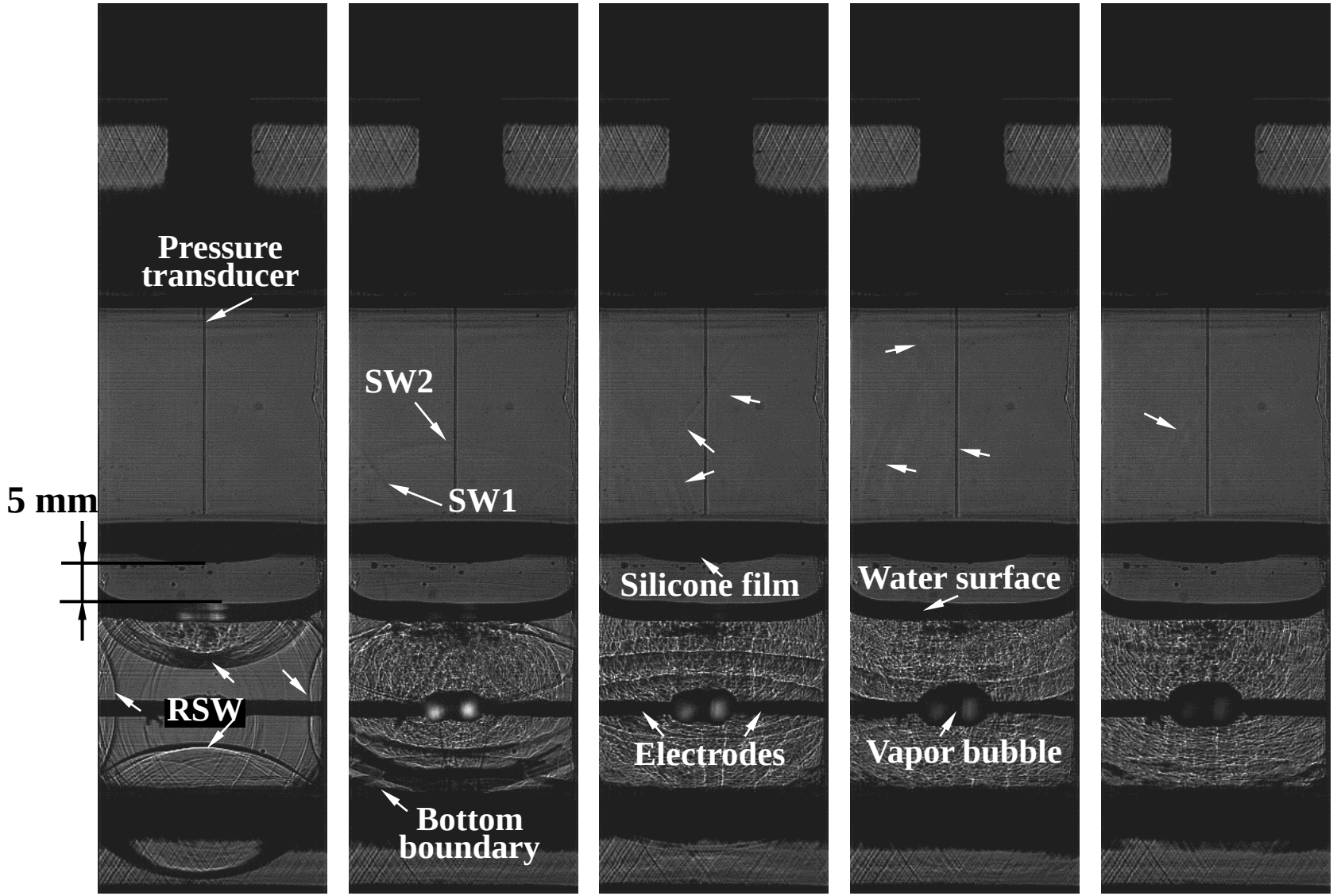
Pressure transducer
SW2
SW1
5 mm
Silicone film
Water surface
RSW
Electrodes
Vapor bubble
Bottom boundary
(1) 10 μs
(2) 20 μs
(3) 30 μs
(4) 40 μs
(5) 50 μs

Fig. 14

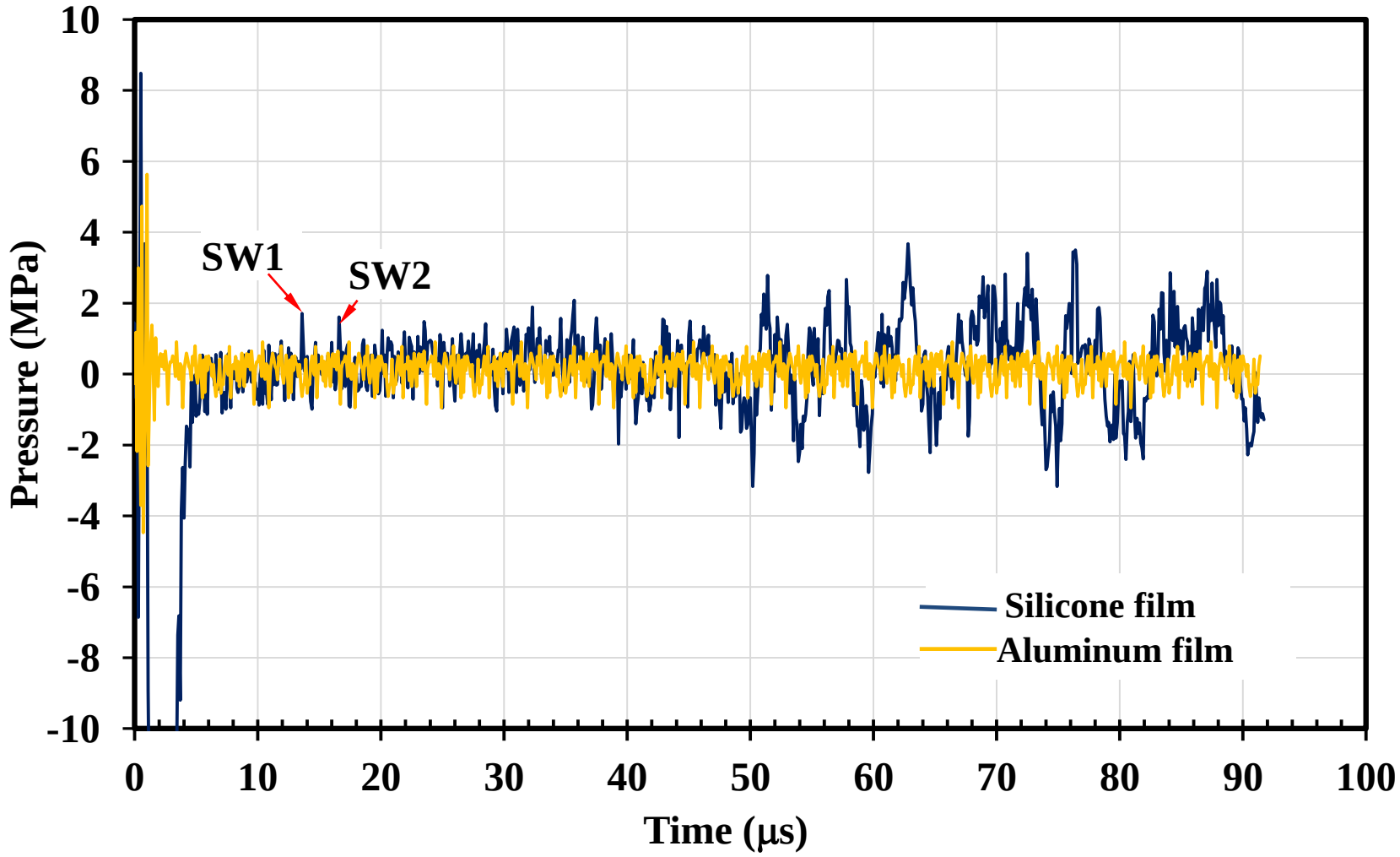
10
8
6
4
2
0
-2
-4
-6
-8
-10
Pressure (MPa)
SW1
SW2
0
10
20
30
40
50
60
70
80
90
100
Time (μs)
Silicone film
Aluminum film

Fig. 15

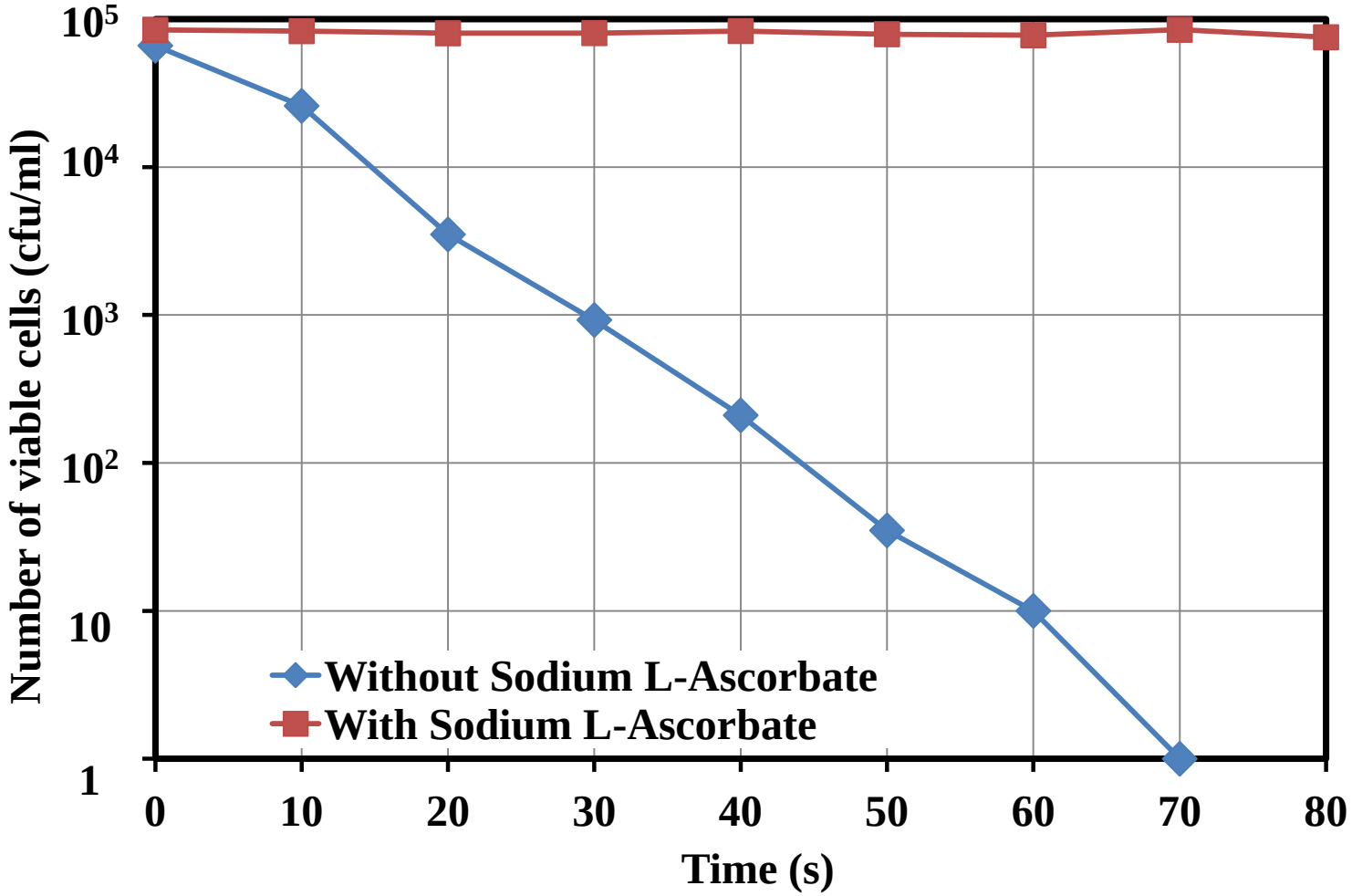
Number of viable cells (cfu/ml)
10^5
10^4
10^3
10^2
10
1
0
10
20
30
40
50
60
70
80
Time (s)
Without Sodium L-Ascorbate
With Sodium L-Ascorbate

Fig. 16

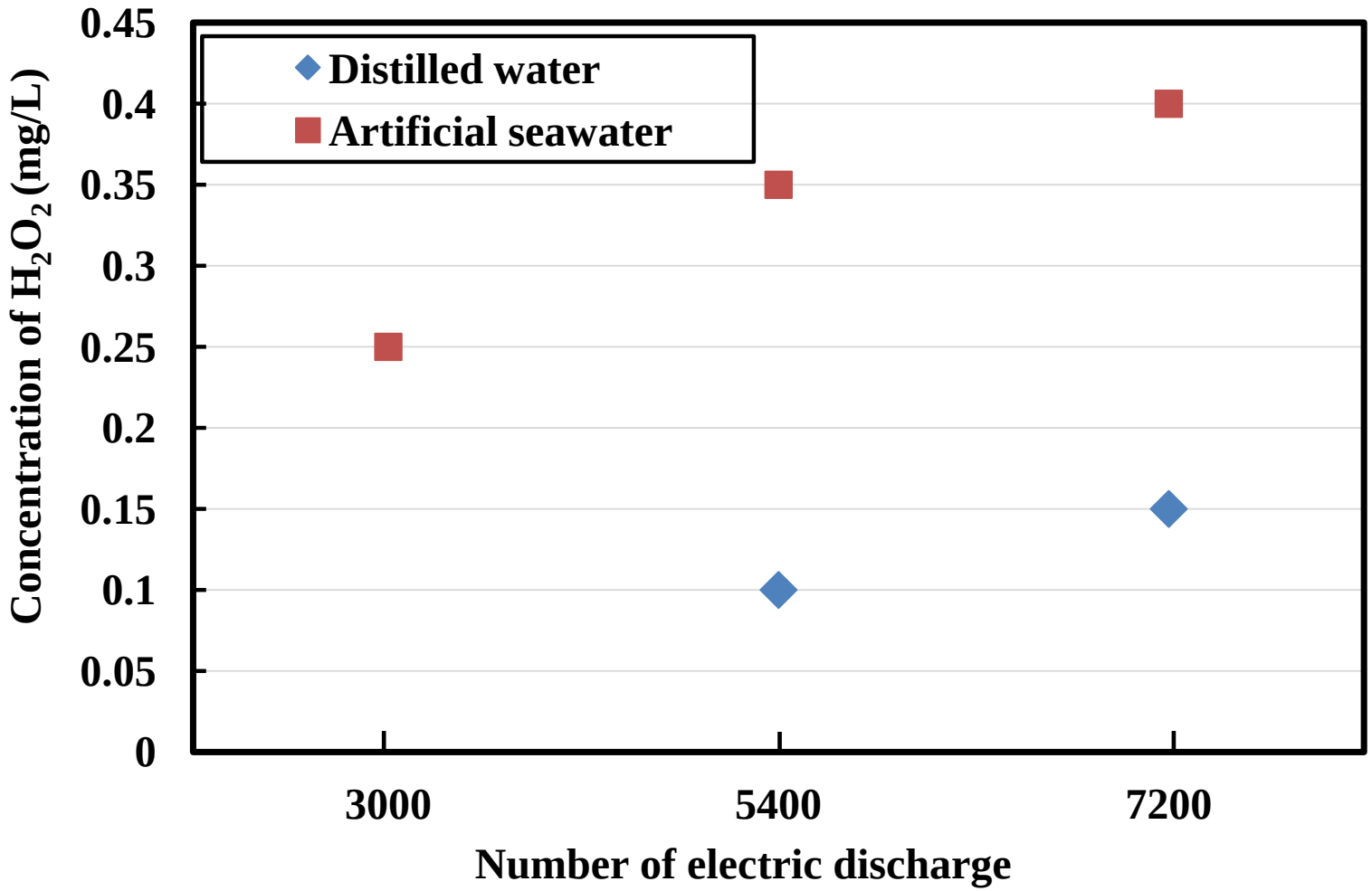

Digital Pack Tester

Fig. 17

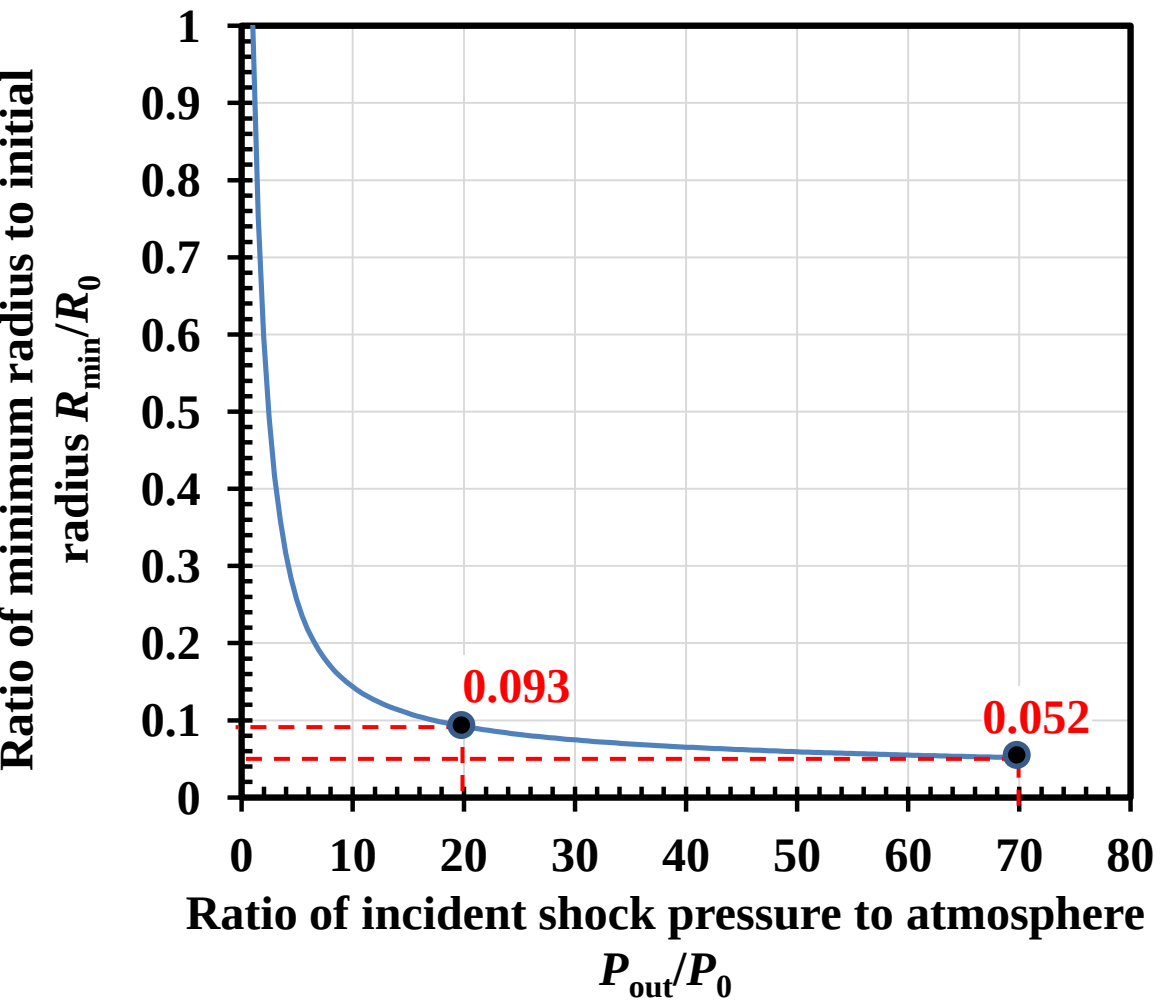
Ratio of minimum radius to initial radius R_{min}/R_0
1
0.9
0.8
0.7
0.6
0.5
0.4
0.3
0.2
0.1
0
0.093
0.052
0
10
20
30
40
50
60
70
80
Ratio of incident shock pressure to atmosphere
P_{out}/P_0

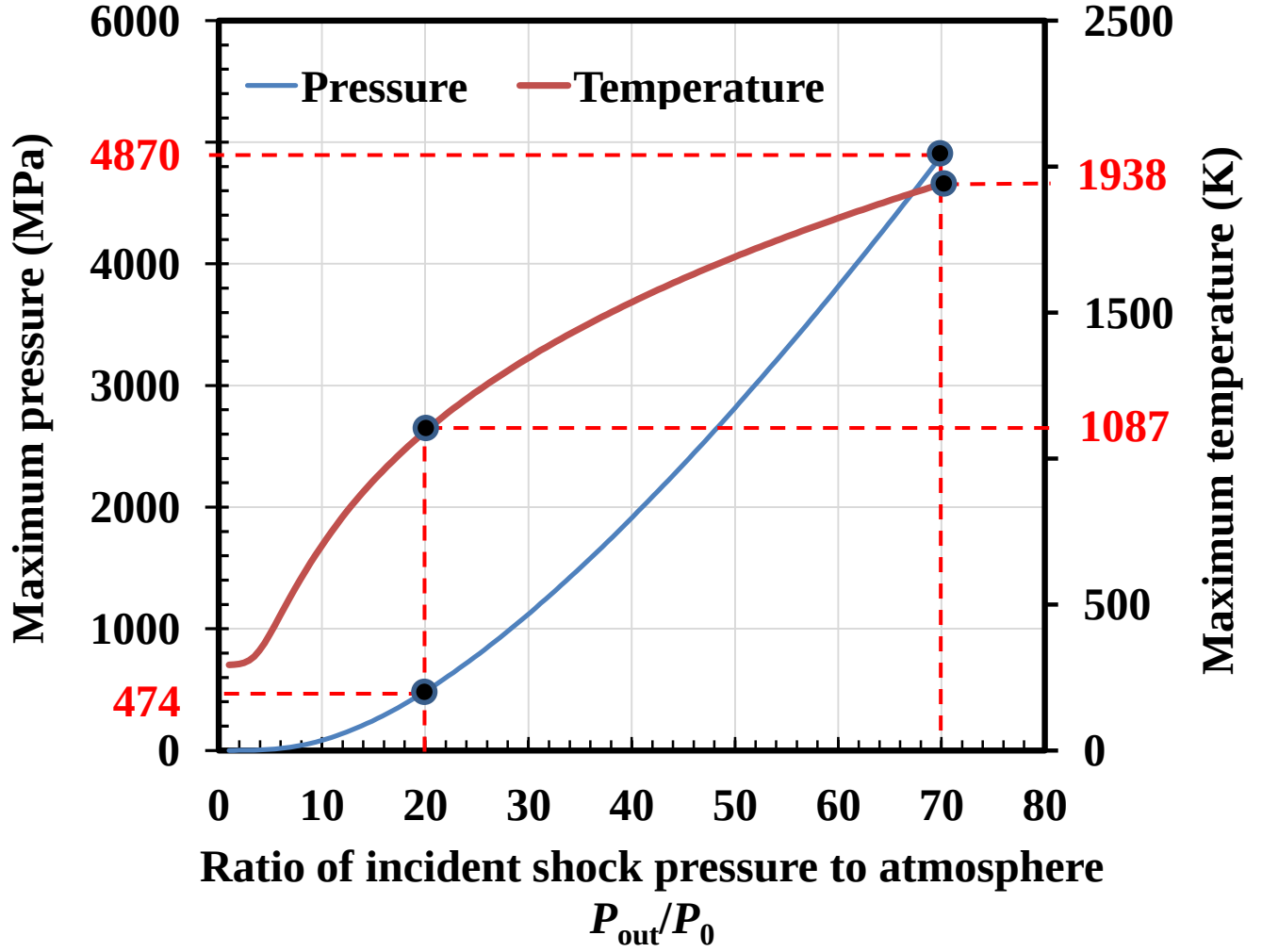
Maximum pressure (MPa)
6000
4870
4000
3000
2000
1000
474
0
Pressure
Temperature
2500
1938
1500
1087
500
0
Maximum temperature (K)
0
10
20
30
40
50
60
70
80
Ratio of incident shock pressure to atmosphere
P_{out}/P_0

Fig. 18

- A high sterilization effect is obtained with supply of only underwater shock waves in a cylindrical water chamber.
- Sterilization effects increases with the strength of bubble motion induced by a shock pressure.
- Free radicals contribute mainly to killing marine bacteria in the case of interaction between large bubbles and weak shock pressures.
- The condition to generate free radicals is investigated theoretically using the Herring equation.